PROCEEDINGS OF SPIE

SPIEDigitalLibrary.org/conference-proceedings-of-spie

Microscopic transport model for impurity scattering in two-dimensional novel a-T3 materials

Huang, D. H., Iurov, A., Xu, H.-Y., Lai, Y.-C., Gumbs, G.

D. H. Huang, A. Iurov, H.-Y. Xu, Y.-C. Lai, G. Gumbs, "Microscopic transport model for impurity scattering in two-dimensional novel a-T3 materials," Proc. SPIE 11129, Infrared Sensors, Devices, and Applications IX, 1112902 (9 September 2019); doi: 10.1117/12.2527782

SPIE.

Event: SPIE Optical Engineering + Applications, 2019, San Diego, California, United States

Microscopic Transport Model for Impurity Scattering in Two-Dimensional Novel α-T_3 Materials

D. H. Huang[1], A. Iurov[2], H.-Y. Xu[3], Y.-C. Lai[3] and G. Gumbs[4]

[1]Air Force Research Laboratory, Space Vehicles Directorate, 3550 Aberdeen Avenue SE, Kirtland Air Force Base, NM 87117, USA

[2]Center for High Technology Materials, University of New Mexico, 1313 Goddard SE, Albuquerque, NM, 87106, USA

[3]School of Electrical, Computer and Energy Engineering, Arizona State University, 650 East Tyler Mall, Tempe, AZ 85287, USA

[4]Department of Physics and Astronomy, Hunter College of CUNY, 695 Park Avenue New York, NY 10065, USA

ABSTRACT

The valley-dependent skew scattering of conduction electrons by impurities in two-dimensional α-T_3 materials is studied. The interplay of Lorentz and Berry forces, which act on mobile electrons in position and momentum spaces respectively, is quantified. Interactions of electrons with ionized impurities at two valleys are observed in different scattering directions. Both the zero- and first-order Boltzmann moment equations are used for calculating scattering-angle distributions of resulting skew currents, which are significantly enhanced by introducing microscopic inverse energy- and momentum-relaxation times to two moment equations.

Keywords: α-T_3 lattices; valley; impurity scattering; momentum relaxation; energy relexation

1. INTRODUCTION

In electronics (spintronics),[1] information is encoded through charge (spin). Valley quantum numbers can also be used to distinguish and designate quantum states of a crystal lattice, which leads to the so-called valleytronics[2,3] and has already attracted a huge amount of interest.[4–10] From physics perspective, valleytronics makes use of controlling the valley degree-of-freedom of certain semiconductor crystals with multiple valleys inside their first Brillouin zone, i.e., band-extreme points. In fact, electron spins have already been used for storing, manipulating and reading out bits of information.[11] As a result, we expect valleytronics will acquire similar functionalities through multiple band extrema, i.e., the so-called bit information could be stored as discrete crystal momenta.

For graphene,[12] its two nonequivalent valleys can be regarded as an ideal two-state system, and its $\boldsymbol{K}$ and $\boldsymbol{K}'$ Dirac points in the first Brillouin zone have distinct momenta or valley

Infrared Sensors, Devices, and Applications IX, edited by Paul D. LeVan, Priyalal Wijewarnasuriya, Ashok K. Sood, Proc. of SPIE Vol. 11129, 1112902

quantum numbers. Since these two valleys are separated by a vary large crystal momentum, we believe them robust against room-temperature external perturbations. Actually, quantum manipulation of valleys has already been demonstrated,[13] in which electrons from different valleys are used for quantum-information processing. Moreover, other two-dimensional materials, i.e., silicene, germanene, MoS_2, WSe_2, also demonstrate similar valley characteristics.

Technically, for valleytronics it is very challenging to separate electrons from two valleys in either position or momentum space, i.e., the so-called valley filters.[14] The valley Hall effect[13] (VHE) can be applied for separating electrons in position space. The other physical phenomena, i.e., the anomalous Hall effect[15] (AHE) and the spin Hall effect[16] (SHE), are expected similar to VHE, where the latter has already shown a connection between the electrical and spin currents for spin-current generation and detection electrically in spintronics. In parallel, we hope VHE will also produce transverse valley currents in position space like SHE.

Theoretically, the α-T_3 physics model is recognized as the newest and best candidate for novel two-dimensional materials. Its obtained low-energy dispersions in this model, including a flat band, can be associated with a three-component generalization, i.e., pseudospin-1 particles, of standard Dirac-Weyl Hamiltonian[17–19] and possess a close relation to graphene.[20–22]

The idea of highly-efficient valley filtering in α-T_3 lattices with a changing Berry phase, as illustrated in Figs. 1(a) and 1(b), has been proposed[23,24] with a Berry-phase-mediated VHE, i.e., gVHE due to the geometric nature of the underlying mechanism. Here, the charge-neutral valley currents appear through skew scattering from ionized impurities at valleys. A physical explanation is offered to resonant valley filtering[25] assisted by skew scattering in order to ensure that gVHE becomes robust against both thermal fluctuations and structural disorders due to a large inter-valley momentum separation.

In this paper, the single-particle quantum-mechanical theory[23] for α-T_3 lattices with variable Berry phases will be generalized to include many-body effects by using Boltzmann transport formalism. This generalized formalism will microscopically compute the inverse energy-relaxation time using the screened second-order Born approximation, the inverse momentum-relaxation-time tensor resulted from scattering by ionized impurities, and the mobility tensor from the force-balance equation. The zeroth- and first-order moment equations from the Boltzmann transport equation will be applied to compute the longitudinal (near-horizontal) and skew-scattering (near-vertical) currents. We will further analyze the competition between Lorentz and Berry forces acting on electrons in position and momentum space, respectively, for non-equilibrium and thermal-equilibrium currents.

2. ELECTRONIC STATES

The single-particle Hamiltonian[17,23] for an α-T_3 lattice has the form of $\overleftrightarrow{\mathcal{H}}_0(\boldsymbol{k}_\parallel) = \hbar v_F \overleftrightarrow{\boldsymbol{\alpha}} \cdot \boldsymbol{k}_\parallel$, where v_F and $\boldsymbol{k}_\parallel = (k_x, k_y)$ are the Fermi velocity and electron wave vector, $\overleftrightarrow{\boldsymbol{\alpha}} = \{\overleftrightarrow{\tau_3} \otimes \overleftrightarrow{S}^{\alpha}_x, \overleftrightarrow{\tau_0} \otimes \overleftrightarrow{S}^{\alpha}_y\}$, $\overleftrightarrow{\tau}_{1,2,3}$ are three Pauli matrices, $\overleftrightarrow{\tau}_0 = \overleftrightarrow{I}_{2\times 2}$ is the identity matrix corresponding to two valleys,

$$\overleftrightarrow{S}^{\alpha}_{x} = \begin{bmatrix} 0 & \cos\phi & 0 \\ \cos\phi & 0 & \sin\phi \\ 0 & \sin\phi & 0 \end{bmatrix} , \qquad \overleftrightarrow{S}^{\alpha}_{y} = \begin{bmatrix} 0 & -i\cos\phi & 0 \\ i\cos\phi & 0 & -i\sin\phi \\ 0 & i\sin\phi & 0 \end{bmatrix} , \tag{1}$$

and $\alpha = \tan\phi$ ($0 \leq \alpha \leq 1$) to parameterize the α-T_3 lattice. For this Hamiltonian, three eigenvalues are given by $\varepsilon_s(k_\parallel) = s\hbar v_F k_\parallel$ with $s = 0, \pm 1$ for three bands. The associated eigenstates are

$$|s, \tau, \boldsymbol{k}_\parallel\rangle_\phi = \frac{1}{\sqrt{2}} \begin{bmatrix} \tau\, \cos\phi\, e^{-i\tau\theta_{\mathbf{k}_\parallel}} \\ s \\ \tau\, \sin\phi\, e^{i\tau\theta_{\mathbf{k}_\parallel}} \end{bmatrix} |\tau\rangle \tag{2}$$

for valley-degenerate eigenvalues $\varepsilon_\pm(k_\parallel) = \pm\,\hbar v_F k_\parallel$ (recorded as (c) for $s = +1$ and (v) for $s = -1$), and

$$|0, \tau, \boldsymbol{k}_\parallel\rangle_\phi = \begin{bmatrix} \tau\, \sin\phi\, e^{-i\tau\theta_{\mathbf{k}_\parallel}} \\ 0 \\ -\tau\, \cos\phi\, e^{i\tau\theta_{\mathbf{k}_\parallel}} \end{bmatrix} |\tau\rangle \tag{3}$$

for $\varepsilon_0(k_\parallel) = 0$, where $\theta_{\mathbf{k}_\parallel} = \tan^{-1}(k_y/k_x)$, and $|\tau = \pm 1\rangle$ represent two different valley states. The Berry connection [26] of each band is defined as the quantum-mechanical average of the position operator $\hat{\boldsymbol{r}}_\parallel = i\hat{\boldsymbol{\nabla}}_{\mathbf{k}_\parallel}$, i.e., $\boldsymbol{A}^{\tau,\phi}_s(\boldsymbol{k}_\parallel) = {}_\phi\langle s, \tau, \boldsymbol{k}_\parallel\, | i\hat{\boldsymbol{\nabla}}_{\mathbf{k}_\parallel} | s, \tau, \boldsymbol{k}_\parallel\rangle_\phi$. As a result, we get from Eqs. (2) and (3) that

$$\boldsymbol{A}^{\tau,\phi}_0(\boldsymbol{k}_\parallel) = -\tau\, \frac{1-\alpha^2}{1+\alpha^2}\, \boldsymbol{\nabla}_{\mathbf{k}_\parallel}\theta_{\mathbf{k}_\parallel} , \qquad \boldsymbol{A}^{\tau,\phi}_s(\boldsymbol{k}_\parallel) = -\frac{1}{2}\, \boldsymbol{A}^{\tau,\phi}_0(\boldsymbol{k}_\parallel) . \tag{4}$$

Moreover, the Berry curvature $\boldsymbol{\Omega}^{\tau,\phi}_s(\boldsymbol{k}_\parallel) = \boldsymbol{\nabla}_{\mathbf{k}_\parallel} \times \boldsymbol{A}^{\tau,\phi}_s(\boldsymbol{k}_\parallel)$ is further calculated as

$$\boldsymbol{\Omega}^{\tau,\phi}_s(\boldsymbol{k}_\parallel) = \tau \left(\frac{1-\alpha^2}{1+\alpha^2}\right) \pi\, \delta(\boldsymbol{k}_\parallel)\, \hat{\boldsymbol{e}}_z , \qquad \boldsymbol{\Omega}^{\tau,\phi}_0(\boldsymbol{k}_\parallel) = -2\, \boldsymbol{\Omega}^{\tau,\phi}_s(\boldsymbol{k}_\parallel) , \tag{5}$$

where $\hat{\boldsymbol{e}}_z$ is the unit coordinate vector in the z direction, perpendicular to α-T_3 plane. Connecting to the Berry connection presented in Eq. (4), the ϕ-dependent Berry phases are calculated as $\Phi^\tau_s(\phi) = \oint d\boldsymbol{k}_\parallel \cdot \boldsymbol{A}^{\tau,\phi}_s(\boldsymbol{k}_\parallel) = \tau\pi\cos 2\phi$ for $s = \pm 1$ and $\Phi^\tau_0(\phi) = -2\Phi^\tau_s(\phi)$. For simplicity, we call the geometry phase ϕ as the "Berry phase" in this paper.

3. IMPURITY SCATTERING

For impurity scattering, the initial $|i\rangle$ and final $|f\rangle$ electron states with wave vectors $\boldsymbol{k}_\parallel$ and $\boldsymbol{k}'_\parallel$ can be written as $|i\rangle = \frac{e^{i\mathbf{k}_\parallel\cdot\mathbf{r}_\parallel}}{\sqrt{\mathcal{S}}}\, |s, \tau, \boldsymbol{k}_\parallel\rangle_\phi$ and $|f\rangle = \frac{e^{i\mathbf{k}'_\parallel\cdot\mathbf{r}_\parallel}}{\sqrt{\mathcal{S}}}\, |s, \tau, \boldsymbol{k}'_\parallel\rangle_\phi$, where $|s, \tau, \boldsymbol{k}_\parallel\rangle_\phi$ is presented in Eq. (2) and $\mathcal{S}$ is the sample area. We assume an isotropic step-like impurity-scattering potential $u^\tau_0(r_\parallel) = \tau V_0\, \Theta(r_0 - r_\parallel)$, where V_0 is the step height, r_0 is the interaction range, and $\tau = +1$

($\tau=-1$) corresponds to a barrier-like (trap-like) potential. Consequently, the screened impurity scattering matrix becomes [27]

$$U_{\rm im}^{\tau,\phi}(\boldsymbol{k}_\parallel',\boldsymbol{k}_\parallel)=\sum_{\mathbf{q}_\parallel'}\frac{U_0^\tau(q_\parallel')}{\epsilon_\phi(q_\parallel')}\,\langle f|e^{i\mathbf{q}_\parallel'\cdot\mathbf{r}_\parallel}|i\rangle=\sum_{\mathbf{q}_\parallel'}\frac{U_0^\tau(q_\parallel')}{\epsilon_\phi(q_\parallel')}$$

$$\times\sum_\ell\langle f|\ell\rangle_{\tau,\phi}\;{}_{\tau,\phi}\langle\ell\,|e^{i\mathbf{q}_\parallel'\cdot\mathbf{r}_\parallel}|i\rangle=\frac{1}{2\mathcal{S}}\sum_{\mathbf{q}_\parallel'}\frac{U_0^\tau(q_\parallel')}{\epsilon_\phi(q_\parallel')}\sum_\ell\int\limits_{r_\parallel'\leq r_0}d^2\boldsymbol{r}_\parallel'\,e^{-i\mathbf{k}_\parallel'\cdot\mathbf{r}_\parallel'}\,\frac{e^{i\ell\Theta_{\mathbf{r}_\parallel'}}}{\sqrt{2\pi}}$$

$$\times\left\{\tau\cos\phi\,e^{-i\tau(\Theta_{\mathbf{r}_\parallel'}-\theta_{\mathbf{k}_\parallel'})}\mathcal{R}_1(r_\parallel')+s\mathcal{R}_2(r_\parallel')+\tau\sin\phi\,e^{i\tau(\Theta_{\mathbf{r}_\parallel'}-\theta_{\mathbf{k}_\parallel'})}\mathcal{R}_3(r_\parallel')\right\}\int\limits_{r_\parallel\leq r_0}d^2\boldsymbol{r}_\parallel\,e^{i(\mathbf{q}_\parallel'+\mathbf{k}_\parallel)\cdot\mathbf{r}_\parallel}$$

$$\times\frac{e^{-i\ell\Theta_{\mathbf{r}_\parallel}}}{\sqrt{2\pi}}\left\{\tau\cos\phi\,e^{i\tau(\Theta_{\mathbf{r}_\parallel}-\theta_{\mathbf{k}_\parallel})}\mathcal{R}_1^*(r_\parallel)+s\mathcal{R}_2^*(r_\parallel)+\tau\sin\phi\,e^{-i\tau(\Theta_{\mathbf{r}_\parallel}-\theta_{\mathbf{k}_\parallel})}\mathcal{R}_3^*(r_\parallel)\right\}\;, \tag{6}$$

where $U_0(q_\parallel')/\epsilon_\phi(q_\parallel')$ is the two-dimensional Fourier transform of the screened impurity potential, and the intermediate quantum states are

$$|\ell\rangle_{\tau,\phi}=\frac{e^{i\ell\Theta_{\mathbf{r}_\parallel}}}{\sqrt{2\pi}}\left[\begin{array}{c}\mathcal{R}_1(r_\parallel)\,e^{-i\tau\Theta_{\mathbf{r}_\parallel}}\\ \mathcal{R}_2(r_\parallel)\\ \mathcal{R}_3(r_\parallel)\,e^{i\tau\Theta_{\mathbf{r}_\parallel}}\end{array}\right]$$

with three radial wave functions for scattered electrons by an ionized impurity atom with a locally-circular symmetry at the valley $|\tau\rangle$. In addition, the first integral with respect to $\boldsymbol{r}_\parallel'$ in Eq. (6) can be evaluated analytically and leads to

$$\text{Integral-}\boldsymbol{r}_\parallel'=\int\limits_0^{r_0}dr_\parallel'\,r_\parallel'\int\limits_0^{2\pi}d\Theta_{\mathbf{r}_\parallel'}\,\frac{e^{i\ell\Theta_{\mathbf{r}_\parallel'}}}{\sqrt{2\pi}}\sum_m J_m(k_\parallel'r_\parallel')\,e^{-im(\theta_{\mathbf{k}_\parallel'}-\Theta_{\mathbf{r}_\parallel'})}\,(-i)^m$$

$$\times\left\{\tau\cos\phi\,e^{-i\tau(\Theta_{\mathbf{r}_\parallel'}-\theta_{\mathbf{k}_\parallel'})}\mathcal{R}_1(r_\parallel')+s\mathcal{R}_2(r_\parallel')+\tau\sin\phi\,e^{i\tau(\Theta_{\mathbf{r}_\parallel'}-\theta_{\mathbf{k}_\parallel'})}\mathcal{R}_3(r_\parallel')\right\}$$

$$=\sqrt{2\pi}(-i)^\ell\,e^{i\ell\theta_{\mathbf{k}_\parallel'}}\int\limits_0^{r_0}dr_\parallel'\,r_\parallel'\left[(-i)^{-\tau}\,\tau\cos\phi\,J_{\ell-\tau}(k_\parallel'r_\parallel')\,\mathcal{R}_1(r_\parallel')\right.$$

$$\left.+sJ_\ell(k_\parallel'r_\parallel')\,\mathcal{R}_2(r_\parallel')+(-i)^\tau\,\tau\sin\phi\,J_{\ell+\tau}(k_\parallel'r_\parallel')\,\mathcal{R}_3(r_\parallel')\right]\;.$$

Similarly, for the second integral with respect to $\boldsymbol{r}_\parallel$ in Eq. (6), we find

$$\text{Integral-}\boldsymbol{r}_\parallel=\int\limits_0^{r_0}dr_\parallel\,r_\parallel\int\limits_0^{2\pi}d\Theta_{\mathbf{r}_\parallel}\,\frac{e^{-i\ell\Theta_{\mathbf{r}_\parallel}}}{\sqrt{2\pi}}\sum_m J_m(|\boldsymbol{k}_\parallel+\boldsymbol{q}_\parallel'|r_\parallel)\,e^{im(\theta_{\mathbf{k}_\parallel+\mathbf{q}_\parallel'}-\Theta_{\mathbf{r}_\parallel})}\,(i)^m$$

$$
\times \left\{ \tau \cos\phi \, e^{i\tau(\Theta_{\mathbf{r}_\parallel} - \theta_{\mathbf{k}_\parallel})} \mathcal{R}_1^*(r_\parallel) + s \mathcal{R}_2^*(r_\parallel) + \tau \sin\phi \, e^{-i\tau(\Theta_{\mathbf{r}_\parallel} - \theta_{\mathbf{k}_\parallel})} \mathcal{R}_3^*(r_\parallel) \right\}
$$

$$
= \sqrt{2\pi} \, (i)^\ell \, e^{-i\ell\theta_{\mathbf{k}_\parallel + \mathbf{q}'_\parallel}} \int_0^{r_0} dr_\parallel \, r_\parallel \left\{ (-i)^\tau \, \tau \cos\phi \, J_{\ell-\tau}(|\boldsymbol{k}_\parallel + \boldsymbol{q}'_\parallel| r_\parallel) \, \mathcal{R}_1^*(r_\parallel) \, e^{i\tau\beta^s_{\mathbf{k}_\parallel, \mathbf{q}'_\parallel}} \right.
$$

$$
\left. + s J_\ell(|\boldsymbol{k}_\parallel + \boldsymbol{q}'_\parallel| r_\parallel) \, \mathcal{R}_2^*(r_\parallel) + (-i)^{-\tau} \, \tau \sin\phi \, J_{\ell+\tau}(|\boldsymbol{k}_\parallel + \boldsymbol{q}'_\parallel| r_\parallel) \, \mathcal{R}_3^*(r_\parallel) \, e^{-i\tau\beta^s_{\mathbf{k}_\parallel, \mathbf{q}'_\parallel}} \right\} \ ,
$$

where $\beta^s_{\mathbf{k}_\parallel, \mathbf{q}'_\parallel} = \theta_{\mathbf{k}_\parallel + \mathbf{q}'_\parallel} - \theta_{\mathbf{k}_\parallel}$ is the scattering angle as illustrated in Fig. 1(c). Finally, by combining these two integrals and putting them into Eq. (6) we arrive at

$$
U^{\tau,\phi}_{\rm im}(\boldsymbol{k}_\parallel + \boldsymbol{q}_\parallel, \boldsymbol{k}_\parallel) = \frac{U_0^\tau(q_\parallel)}{\epsilon_\phi(q_\parallel) \, \mathcal{S}} \, \mathcal{F}_{\tau,\phi}(\boldsymbol{k}_\parallel, \boldsymbol{q}_\parallel) \ , \tag{7}
$$

where the scattering form factor $\mathcal{F}_{\tau,\phi}(\boldsymbol{k}_\parallel, \boldsymbol{q}_\parallel)$ is defined as

$$
\mathcal{F}_{\tau,\phi}(\boldsymbol{k}_\parallel, \boldsymbol{q}_\parallel) = \frac{1}{2} \sum_\ell \left\{ (-i)^{-\tau} \tau \cos\phi \, \chi_1(|\boldsymbol{k}_\parallel + \boldsymbol{q}_\parallel|) + s \chi_2(|\boldsymbol{k}_\parallel + \boldsymbol{q}_\parallel|) \right.
$$

$$
\left. + (-i)^\tau \tau \sin\phi \, \chi_3(|\boldsymbol{k}_\parallel + \boldsymbol{q}_\parallel|) \right\} \left\{ (-i)^\tau \tau \cos\phi \, \chi_1^*(|\boldsymbol{k}_\parallel + \boldsymbol{q}_\parallel|) \, e^{i\tau\beta^s_{\mathbf{k}_\parallel, \mathbf{q}_\parallel}} + s \chi_2^*(|\boldsymbol{k}_\parallel + \boldsymbol{q}_\parallel|) \right.
$$

$$
\left. + (-i)^{-\tau} \tau \sin\phi \, \chi_3^*(|\boldsymbol{k}_\parallel + \boldsymbol{q}_\parallel|) \, e^{-i\tau\beta^s_{\mathbf{k}_\parallel, \mathbf{q}_\parallel}} \right\} \ . \tag{8}
$$

Here, we have introduced in Eq. (8) the following three complex functions

$$
\left\{ \begin{array}{c} \chi_1(|\boldsymbol{k}_\parallel + \boldsymbol{q}_\parallel|) \\ \chi_2(|\boldsymbol{k}_\parallel + \boldsymbol{q}_\parallel|) \\ \chi_3(|\boldsymbol{k}_\parallel + \boldsymbol{q}_\parallel|) \end{array} \right\} = \sqrt{2\pi} \int_0^{r_0} dr_\parallel \, r_\parallel \left\{ \begin{array}{c} J_{\ell-\tau}(|\boldsymbol{k}_\parallel + \boldsymbol{q}_\parallel| r_\parallel) \, \mathcal{R}_1(r_\parallel) \\ J_\ell(|\boldsymbol{k}_\parallel + \boldsymbol{q}_\parallel| r_\parallel) \, \mathcal{R}_2(r_\parallel) \\ J_{\ell+\tau}(|\boldsymbol{k}_\parallel + \boldsymbol{q}_\parallel| r_\parallel) \, \mathcal{R}_3(r_\parallel) \end{array} \right\} \ . \tag{9}
$$

4. DIELECTRIC FUNCTION

Under the random-phase approximation ,[28] the dielectric function $\epsilon_\phi(q_\parallel, \omega)$ for α-T_3 lattices is found to be

$$
\epsilon_\phi(q_\parallel, \omega) = 1 + \left(\frac{e^2}{2\epsilon_0 \epsilon_{\rm r} q_\parallel} \right) \mathcal{Q}_\phi(q_\parallel, \omega) \ , \tag{10}
$$

where the polarization function $\mathcal{Q}_\phi(q_\parallel, \omega)$ is defined as

$$
\mathcal{Q}_\phi(q_\parallel, \omega) = \frac{2}{\mathcal{S}} \sum_{\tau, \mathbf{k}_\parallel, s, s'} \mathcal{G}^{\tau,\phi}_{s,s'}(\boldsymbol{k}_\parallel, \boldsymbol{q}_\parallel) \left\{ \frac{f_T^{(0)}[\varepsilon_{s'}(|\boldsymbol{k}_\parallel + \boldsymbol{q}_\parallel|)] - f_T^{(0)}[\varepsilon_s(k_\parallel)]}{\hbar(\omega + i0^+) - \varepsilon_{s'}(|\boldsymbol{k}_\parallel + \boldsymbol{q}_\parallel|) + \varepsilon_s(k_\parallel)} \right\} \ . \tag{11}
$$

The prefactor 2 in Eq. (11) comes from the spin degeneracy, $\mathcal{S}$ is the sample area, $\varepsilon_s(k_\parallel) = s\hbar v_F k_\parallel$ with $s = 0, \pm 1$, ω is the angular frequency of a probe field, $f_T^{(0)}(x) = \{1 + \exp[(x - u_0)/k_B T]\}^{-1}$

is the Fermi function for thermal-equilibrium electrons, $u_0(T)$ is the electron chemical potential, and T is the temperature. The overlap function $\mathcal{G}^{\tau,\phi}_{s,s'}(\boldsymbol{k}_\parallel,\boldsymbol{q}_\parallel)$ in Eq. (11) for different electronic states is

$$\mathcal{G}^{\tau,\phi}_{s,s'}(\boldsymbol{k}_\parallel,\boldsymbol{q}_\parallel)=\mathcal{G}^{\tau,\phi}_{s',s}(\boldsymbol{q}_\parallel,\boldsymbol{k}_\parallel)=\left|{}_\phi\Big\langle s,\tau,\boldsymbol{k}_\parallel\Big|s',\tau,\boldsymbol{k}_\parallel+\boldsymbol{q}_\parallel\Big\rangle_\phi\right|^2\ ,\tag{12}$$

and the wave functions $|s,\tau,\boldsymbol{k}_\parallel\rangle_\phi$ for $s=0,\pm1$ and $\tau=\pm1$ are shown in Eqs. (2) and (3). For $k_BT\ll E_F$, the remaining nonzero terms in Eq. (11) in the summation over s and s' correspond to $s'=+1$, $s=0,\pm1$, or vice versa. As a result, we get three finite terms [18] from Eq. (12), i.e.,

$$\mathcal{G}^{\tau,\phi}_{0,+1}(\boldsymbol{k}_\parallel,\boldsymbol{q}_\parallel)=\frac{1}{2}\ \sin^2(2\phi)\ \sin^2(\beta^s_{\mathbf{k}_\parallel,\mathbf{q}_\parallel})\ ,\tag{13}$$

$$\mathcal{G}^{\tau,\phi}_{\pm1,+1}(\boldsymbol{k}_\parallel,\boldsymbol{q}_\parallel)=\frac{1}{4}\ \Big\{1\pm\cos(\beta^s_{\mathbf{k}_\parallel,\mathbf{q}_\parallel})\Big\}^2+\frac{1}{4}\ \cos^2(2\phi)\ \sin^2(\beta^s_{\mathbf{k}_\parallel,\mathbf{q}_\parallel})\ ,\tag{14}$$

which become independent of τ, where $\beta^s_{\mathbf{k}_\parallel,\mathbf{q}_\parallel}=\theta_{\mathbf{k}_\parallel+\mathbf{q}_\parallel}-\theta_{\mathbf{k}_\parallel}$ is the angle between wave vectors $\boldsymbol{k}_\parallel$ and $\boldsymbol{k}_\parallel+\boldsymbol{q}_\parallel$, and $\theta_{\mathbf{k}_\parallel}=\tan^{-1}(k_y/k_x)$ is the angle between $\boldsymbol{k}_\parallel$ and x-axis.

Setting $\omega=0$, we get the static dielectric function $\epsilon_\phi(q_\parallel)$ from Eq. (10) by using

$$\mathcal{Q}_\phi(q_\parallel,\omega=0)=a_\phi(q_\parallel)+\Theta(q_\parallel-2k_F)\,b_\phi(q_\parallel)\ ,\tag{15}$$

where $k_F=\sqrt{\pi\rho_0}$ and ρ_0 is the areal electron density. If $q_\parallel<2k_F$ is further assumed, we find $q_\phi=(e^2/2\epsilon_0\epsilon_r)\,a_\phi(q_\parallel)\approx(e^2k_F)/(\pi\epsilon_0\epsilon_r\hbar v_F)$ for $\epsilon_\phi(q_\parallel)=1+q_\phi/q_\parallel$. As $q_\parallel\ll k_F$, $a_\phi(q_\parallel)$ becomes independent of ϕ and is given by [18]

$$a_\phi(q_\parallel)=\frac{1}{2\pi\hbar v_F}\ \left(4k_F+\frac{q_\parallel^2}{k_F}\right)\approx\frac{2k_F}{\pi\hbar v_F}\ .\tag{16}$$

5. ENERGY-RELAXATION TIME

Under the detailed-balance condition, the microscopic energy-relaxation time $\tau_\phi(\boldsymbol{k}_\parallel,\tau)$ in Eq. (42) can be calculated from [35]

$$\frac{1}{\tau_\phi(\boldsymbol{k}_\parallel,\tau)}=\mathcal{W}^{\tau,\phi}_{\rm in}(\boldsymbol{k}_\parallel)+\mathcal{W}^{\tau,\phi}_{\rm out}(\boldsymbol{k}_\parallel)\ ,\tag{17}$$

where the scattering-in rate for electrons in the final $\boldsymbol{k}_\parallel$-state is

$$\mathcal{W}^{\tau,\phi}_{\rm in}(\boldsymbol{k}_\parallel)=\frac{\pi N_i}{\hbar}\ \sum_{\mathbf{q}_\parallel}\ \left|U^{\tau,\phi}_{\rm im}(\boldsymbol{q}_\parallel,\boldsymbol{k}_\parallel)\right|^2\ \Big\{f_{\mathbf{k}_\parallel-\mathbf{q}_\parallel}\,\delta(\varepsilon_{\mathbf{k}_\parallel}-\varepsilon_{\mathbf{k}_\parallel-\mathbf{q}_\parallel})+f_{\mathbf{k}_\parallel+\mathbf{q}_\parallel}\,\delta(\varepsilon_{\mathbf{k}_\parallel}-\varepsilon_{\mathbf{k}_\parallel+\mathbf{q}_\parallel})\Big\}\ ,\tag{18}$$

and its scattering-out rate in the initial $\boldsymbol{k}_\parallel$-state is

$$
\mathcal{W}^{\tau,\phi}_{\rm out}(\boldsymbol{k}_\parallel)=\frac{\pi N_i}{\hbar}\sum_{\mathbf{q}_\parallel}\left|U^{\tau,\phi}_{\rm im}(\boldsymbol{q}_\parallel,\boldsymbol{k}_\parallel)\right|^2\,\Big\{(1-f_{\mathbf{k}_\parallel+\mathbf{q}_\parallel})\,\delta(\varepsilon_{\mathbf{k}_\parallel+\mathbf{q}_\parallel}-\varepsilon_{\mathbf{k}_\parallel})
+(1-f_{\mathbf{k}_\parallel-\mathbf{q}_\parallel})\,\delta(\varepsilon_{\mathbf{k}_\parallel-\mathbf{q}_\parallel}-\varepsilon_{\mathbf{k}_\parallel})\Big\}\ . \tag{19}
$$

For simplicity, we have introduced the notations $f_{\mathbf{k}_\parallel}\equiv f^{(0)}_T[\varepsilon(k_\parallel)]$ and $\varepsilon_{\mathbf{k}_\parallel}\equiv\varepsilon_+(k_\parallel)$. We have also assumed $k_BT\ll E_F$ and low ρ_0 so that both electron-phonon and electron-pair scattering can be neglected compared with dominant impurity scattering. N_i is the number of ionized impurities in the system, and $\left|U^{\tau,\phi}_{\rm im}(\boldsymbol{q}_\parallel,\boldsymbol{k}_\parallel)\right|^2$ can be obtained from the the second-order Born approximation.

Using the results in Sec. 3, we arrive at the screened impurity scattering interaction, given by

$$
\left|U^{\tau,\phi}_{\rm im}(\boldsymbol{q}_\parallel,\,\boldsymbol{k}_\parallel)\right|^2=\left|\frac{U^\tau_0(q_\parallel)}{\epsilon_\phi(q_\parallel)\,\mathcal{S}}\right|^2\left|\mathcal{F}_{\tau,\phi}(\boldsymbol{k}_\parallel,\boldsymbol{q}_\parallel)\right|^2\ , \tag{20}
$$

where $\mathcal{S}$ is the sample area, and $\epsilon_\phi(q_\parallel)$ is a static dielectric function determined from Eqs. (10) and (15). Here, the scattering form factor $\mathcal{F}_{\tau,\phi}(\mathbf{k}_\parallel,\mathbf{q}_\parallel)$ is

$$
\mathcal{F}_{\tau,\phi}(\boldsymbol{k}_\parallel,\boldsymbol{q}_\parallel)=\frac{1}{2}\sum_\ell\big\{(-i)^{-\tau}\tau\cos\phi\,\chi_1(|\boldsymbol{k}_\parallel+\boldsymbol{q}_\parallel|)+s\chi_2(|\boldsymbol{k}_\parallel+\boldsymbol{q}_\parallel|)
+(-i)^{\tau}\tau\sin\phi\,\chi_3(|\boldsymbol{k}_\parallel+\boldsymbol{q}_\parallel|)\big\}\Big\{(-i)^{\tau}\tau\cos\phi\,\chi^*_1(|\boldsymbol{k}_\parallel+\boldsymbol{q}_\parallel|)\,e^{i\tau\beta^s_{\mathbf{k}_\parallel,\mathbf{q}_\parallel}}+s\chi^*_2(|\boldsymbol{k}_\parallel+\boldsymbol{q}_\parallel|)
+(-i)^{-\tau}\tau\sin\phi\,\chi^*_3(|\boldsymbol{k}_\parallel+\boldsymbol{q}_\parallel|)\,e^{-i\tau\beta^s_{\mathbf{k}_\parallel,\mathbf{q}_\parallel}}\Big\}\ , \tag{21}
$$

where $s=+1$ is selected for electrons, $\tau=\pm1$ for two inequivalent valleys, $\alpha=\tan\phi$, $\beta^s_{\mathbf{k}_\parallel,\mathbf{q}_\parallel}\equiv\theta_{\mathbf{k}_\parallel+\mathbf{q}_\parallel}-\theta_{\mathbf{k}_\parallel}$, and $\theta_{\mathbf{k}_\parallel}=\tan^{-1}(k_y/k_x)$. We define the scattering factors $\chi_n(|\boldsymbol{k}_\parallel+\boldsymbol{q}_\parallel|)$ with $n=1,\,2,\,3$ in Eq. (21) as

$$
\frac{1}{\sqrt{2\pi}}\left\{\begin{array}{c}\chi_1(|\boldsymbol{k}_\parallel+\boldsymbol{q}_\parallel|)\\ \chi_2(|\boldsymbol{k}_\parallel+\boldsymbol{q}_\parallel|)\\ \chi_3(|\boldsymbol{k}_\parallel+\boldsymbol{q}_\parallel|)\end{array}\right\}=\left\{\int\limits_0^1 d\xi\,\xi\left(|\mathcal{R}_1(\xi)|^2+|\mathcal{R}_2(\xi)|^2+|\mathcal{R}_3(\xi)|^2\right)\right\}^{-1/2}
\times\int\limits_0^1 d\xi\,\xi\left\{\begin{array}{c}J_{\ell-\tau}(|\boldsymbol{k}_\parallel+\boldsymbol{q}_\parallel|r_0\xi)\,\mathcal{R}_1(\xi)\\ J_\ell(|\boldsymbol{k}_\parallel+\boldsymbol{q}_\parallel|r_0\xi)\,\mathcal{R}_2(\xi)\\ J_{\ell+\tau}(|\boldsymbol{k}_\parallel+\boldsymbol{q}_\parallel|r_0\xi)\,\mathcal{R}_3(\xi)\end{array}\right\}\ , \tag{22}
$$

where $J_\ell(x)$ is the Bessel function of the first kind, ℓ is the angular-momentum quantum number and r_0 represents the range of impurity interaction. The radial wave functions $\mathcal{R}_n(\xi)$ for $n=1,\,2,\,3$ in Eq. (22) satisfy the matrix-form Dirac equation for massless three-component generalization of Dirac-Weyl particles,[23] i.e.,

$$
\begin{bmatrix}
u_0^\tau(\xi) & -\frac{i\tau\hbar v_F\cos\phi}{r_0}\left(\frac{d}{d\xi}+\frac{\tau\ell}{\xi}\right) & 0 \\
-\frac{i\tau\hbar v_F\cos\phi}{r_0}\left(\frac{d}{d\xi}-\frac{\tau(\ell-\tau)}{\xi}\right) & u_0^\tau(\xi) & -\frac{i\tau\hbar v_F\sin\phi}{r_0}\left(\frac{d}{d\xi}+\frac{\tau(\ell+\tau)}{\xi}\right) \\
0 & -\frac{i\tau\hbar v_F\sin\phi}{r_0}\left(\frac{d}{d\xi}-\frac{\tau\ell}{\xi}\right) & u_0^\tau(\xi)
\end{bmatrix}
$$

$$
\bigotimes \begin{bmatrix} \mathcal{R}_1(\xi) \\ \mathcal{R}_2(\xi) \\ \mathcal{R}_3(\xi) \end{bmatrix} = E_0(k_\parallel) \begin{bmatrix} \mathcal{R}_1(\xi) \\ \mathcal{R}_2(\xi) \\ \mathcal{R}_3(\xi) \end{bmatrix} , \tag{23}
$$

where $E_0(k_\parallel)$ is the kinetic energy for incident electrons, $u_0^\tau(\xi) = \tau V_0\,\Theta(1-\xi)$ is a barrier-like ($\tau = +1$) or a trap-like ($\tau = -1$) impurity potential, and V_0 is a potential-step height within the region of $0 \leq \xi = r/r_0 \leq 1$. The Fourier transform of the scattering potential $u_0^\tau(\xi)$ in Eq. (23) takes the form

$$
U_0^\tau(q_\parallel) = \tau V_0(2\pi r_0^2) \int_0^1 d\xi\, \xi\, J_0(\xi r_0 q_\parallel) \; . \tag{24}
$$

If $\phi \neq \pi/4$, we find from Eqs. (21)-(23) that $\mathcal{F}_{\tau,\phi}(\boldsymbol{k}_\parallel, \boldsymbol{q}_\parallel) \neq \mathcal{F}_{-\tau,\phi}(\boldsymbol{k}_\parallel, \boldsymbol{q}_\parallel)$ and $\chi_1(|\boldsymbol{k}_\parallel + \boldsymbol{q}_\parallel|) \neq \chi_3(|\boldsymbol{k}_\parallel + \boldsymbol{q}_\parallel|)$, leading to valley-dependent impurity scattering. This results from a switching from the translational symmetry in a crystal to locally-rotational symmetry around an impurity atom., and from the valley-dependent barrier- or trap-like impurity potential as well. Equation (23) can be solved analytically [23] for an electron interacting with an ionized impurity atom, giving rise to

$$
\begin{bmatrix} \mathcal{R}_{1,\ell}^\tau(\xi) \\ \mathcal{R}_{2,\ell}^\tau(\xi) \\ \mathcal{R}_{3,\ell}^\tau(\xi) \end{bmatrix} = \begin{bmatrix} \cos\phi\, J_{\ell-\tau}(\xi\eta_0^\tau) \\ iS_0^\tau\, J_\ell(\xi\eta_0^\tau) \\ -\sin\phi\, J_{\ell+\tau}(\xi\eta_0^\tau) \end{bmatrix} , \tag{25}
$$

where $\eta_0^\tau(k_\parallel) = |E_0(k_\parallel) - \tau V_0| r_0/\hbar v_F$, and $S_0^\tau = \text{sgn}(E_0(k_\parallel) - \tau V_0)$ with $(S_0^\tau)^2 = 1$.

From Eq. (18) we find

$$
\mathcal{W}_{\rm in}^{\tau,\phi}(k_\parallel) = \frac{n_i}{2\pi\hbar^2 v_F}\, k_\parallel f_{k_\parallel} \sum_\pm \int_{-\pi}^{\pi} d\beta_s\, |\cos\theta| \left| \frac{U_0^\tau(2k_\parallel|\cos\theta|)}{\epsilon_\phi(2k_\parallel|\cos\theta|)} \right|^2 |\mathcal{F}_{\tau,\phi}(k_\parallel, \beta_s)|^2 \; , \tag{26}
$$

where $|\cos\theta| = |\sin(|\beta_s|/2)|$, $n_i = N_i/\mathcal{S}$ is the areal density of ionized impurities, and the summation $\sum\limits_\pm$ is associated with $\varepsilon_{\mathbf{k}_\parallel} = \varepsilon_{\mathbf{k}_\parallel \pm \mathbf{q}_\parallel}$ for two delta-functions in Eq. (18). From Eq. (21) we further find

$$
\mathcal{F}_{\tau,\phi}(k_\parallel, \beta_s) = \frac{1}{2} \sum_\ell \left\{ (-i)^{-\tau}\tau\cos\phi\, \chi_{1,\ell}^\tau(k_\parallel) + \chi_{2,\ell}^\tau(k_\parallel) + (-i)^\tau \tau \sin\phi\, \chi_{3,\ell}^\tau(k_\parallel) \right\}
$$

$$\times\left\{(-i)^\tau\tau\cos\phi\,\chi^\tau_{1,\ell}(k_\|)\,e^{i\tau\beta^s_{\mathbf{k}_\|,\mathbf{q}_\|}}-\chi^\tau_{2,\ell}(k_\|)+(-i)^{-\tau}\tau\sin\phi\,\chi^\tau_{3,\ell}(k_\|)\,e^{-i\tau\beta^s_{\mathbf{k}_\|,\mathbf{q}_\|}}\right\}$$
$$\equiv\kappa_0(k_\|,\phi,\tau)+\kappa_1(k_\|,\phi,\tau)\,e^{i\tau\beta_s}+\kappa_2(k_\|,\phi,\tau)\,e^{-i\tau\beta_s}+\kappa_3(k_\|,\phi,\tau)(1+e^{i\tau\beta_s})$$
$$+\kappa_4(k_\|,\phi,\tau)(1+e^{-i\tau\beta_s})+\kappa_5(k_\|,\phi,\tau)\cos(\tau\beta_s)\ , \tag{27}$$

where

$$\left\{\begin{array}{l}\chi^\tau_{1,\ell}(k_\|)\\ \chi^\tau_{2,\ell}(k_\|)\\ \chi^\tau_{3,\ell}(k_\|)\end{array}\right\}=\sqrt{2\pi}\left\{\int_0^1 d\xi\,\xi\left[\cos^2\phi J^2_{\ell-\tau}(\xi\eta^\tau_0)+J^2_\ell(\xi\eta^\tau_0)+\sin^2\phi J^2_{\ell+\tau}(\xi\eta^\tau_0)\right]\right\}^{-1/2}$$
$$\times\left\{\begin{array}{l}\cos\phi\\ iS^\tau_0\\ -\sin\phi\end{array}\right\}\int_0^1 d\xi\,\xi\left\{\begin{array}{l}J_{\ell-\tau}(k_\|r_0\xi)J_{\ell-\tau}(\xi\eta^\tau_0)\\ J_\ell(k_\|r_0\xi)J_\ell(\xi\eta^\tau_0)\\ J_{\ell+\tau}(k_\|r_0\xi)J_{\ell+\tau}(\xi\eta^\tau_0)\end{array}\right\}\ , \tag{28}$$

and six real coefficients κ_i for $i=0,\,1,\cdots,\,5$ are defined as

$$\begin{aligned}
\kappa_0(k_\|,\phi,\tau)&=\frac{1}{2}\sum_{\ell=-\infty}^{\infty}\left|\chi^\tau_{2,\ell}(k_\|)\right|^2\ ,\\
\kappa_1(k_\|,\phi,\tau)&=\frac{1}{2}\cos^2\phi\sum_{\ell=-\infty}^{\infty}\left[\chi^\tau_{1,\ell}(k_\|)\right]^2\ ,\\
\kappa_2(k_\|,\phi,\tau)&=\frac{1}{2}\sin^2\phi\sum_{\ell=-\infty}^{\infty}\left[\chi^\tau_{3,\ell}(k_\|)\right]^2\ ,\\
\kappa_3(k_\|,\phi,\tau)&=-\frac{i}{2}\cos\phi\sum_{\ell=-\infty}^{\infty}\chi^\tau_{1,\ell}(k_\|)\chi^\tau_{2,\ell}(k_\|)\ ,\\
\kappa_4(k_\|,\phi,\tau)&=+\frac{i}{2}\sin\phi\sum_{\ell=-\infty}^{\infty}\chi^\tau_{2,\ell}(k_\|)\chi^\tau_{3,\ell}(k_\|)\ ,\\
\kappa_5(k_\|,\phi,\tau)&=-\frac{1}{2}\sin 2\phi\sum_{\ell=-\infty}^{\infty}\chi^\tau_{1,\ell}(k_\|)\chi^\tau_{3,\ell}(k_\|)\ .
\end{aligned}\tag{29}$$

For $k_BT\ll E_F$, from the detailed-balance condition and Eq. (26) we obtain the energy-relaxation rate

$$\frac{1}{\bar{\tau}_\phi(k_F,\tau)}=\frac{4}{\rho_0\mathcal{S}}\sum_{\mathbf{k}_\|}\frac{f^{(0)}_T[\varepsilon(k_\|)]}{\tau_\phi(\boldsymbol{k}_\|,\tau)}=\frac{4}{\rho_0\mathcal{S}}\sum_{\mathbf{k}_\|}\mathcal{W}^{\tau,\phi}_{\rm in}(k_\|)\,\Theta(k_F-k_\|)$$
$$=\frac{4n_i}{\pi^2\hbar^2v_F\rho_0}\int_{-\pi}^{\pi}d\beta_s\,|\cos\theta|\int_0^{k_F}dk_\|\,k_\|^2\left|\frac{U^\tau_0(2k_\||\cos\theta|)}{\epsilon_\phi(2k_\||\cos\theta|)}\right|^2|\mathcal{F}_{\tau,\phi}(k_\|,\beta_s)|^2\ . \tag{30}$$

6. MOMENTUM-RELAXATION-TIME

The inverse momentum-relaxation-time tensor $\overleftrightarrow{\mathcal{T}}_p^{-1}(\tau,\phi)$ in Eq. (44) can be calculated using the average resistive forces $\boldsymbol{f}(\tau,\phi)$ in the presence of electron scattering by ionized impurities under $k_BT \ll E_F$.[31,32]

For electrons moving with a center-of-mass momentum $\hbar\boldsymbol{K}_0^{\tau,\phi}$, the resistive force $\boldsymbol{f}(\tau,\phi)$ from impurity scattering is[35]

$$\boldsymbol{f}(\tau,\phi) = -N_i\left(\frac{2\pi}{\hbar}\right)\frac{v_F}{k_F}\sum_{\mathbf{k}_\parallel,\mathbf{q}_\parallel}\hbar\boldsymbol{q}_\parallel\left(\hbar\boldsymbol{q}_\parallel\cdot\boldsymbol{K}_0^{\tau,\phi}\right)$$
$$\times\left|U_{\rm im}^{\tau,\phi}(\boldsymbol{q}_\parallel,\,\boldsymbol{k}_\parallel)\right|^2\left(-\frac{\partial f_{\mathbf{k}_\parallel}}{\partial\varepsilon_{\mathbf{k}_\parallel}}\right)\delta(\varepsilon_{\mathbf{k}_\parallel+\mathbf{q}_\parallel}-\varepsilon_{\mathbf{k}_\parallel})\ . \tag{31}$$

Using the definition $\overleftrightarrow{\mathcal{T}}_p^{-1}(\tau,\phi)\cdot\boldsymbol{K}_0^{\tau,\phi} = -\boldsymbol{f}(\tau,\phi)/N_0\hbar$, we get

$$\overleftrightarrow{\mathcal{T}}_p^{-1}(\tau,\phi) = \frac{2\pi N_i v_F}{N_0 k_F}\sum_{\mathbf{k}_\parallel,\mathbf{q}_\parallel}\left|U_{\rm im}^{\tau,\phi}(\boldsymbol{q}_\parallel,\,\boldsymbol{k}_\parallel)\right|^2\left(-\frac{\partial f_{\mathbf{k}_\parallel}}{\partial\varepsilon_{\mathbf{k}_\parallel}}\right)\delta(\varepsilon_{\mathbf{k}_\parallel+\mathbf{q}_\parallel}-\varepsilon_{\mathbf{k}_\parallel})\,\left[\boldsymbol{q}_\parallel\otimes\boldsymbol{q}_\parallel^T\right]\ , \tag{32}$$

where the notation

$$\left[\boldsymbol{q}_\parallel\otimes\boldsymbol{q}_\parallel^T\right] \equiv \left[\begin{array}{cc} q_x^2 & q_xq_y \\ q_yq_x & q_y^2\end{array}\right]\ .$$

For $k_BT \ll E_F$, from Eqs. (31) and (32) we have

$$\overleftrightarrow{\mathcal{T}}_p^{-1}(k_F,\tau,\phi) = \frac{2\pi n_i}{\rho_0}\left(\frac{v_F}{k_F}\right)\sum_{\mathbf{k}_\parallel,\mathbf{q}_\parallel}\left|U_{\rm im}^{\tau,\phi}(\boldsymbol{q}_\parallel,\,\boldsymbol{k}_\parallel)\right|^2\delta(\varepsilon_{\mathbf{k}_\parallel}-E_F)\,\delta(\varepsilon_{\mathbf{k}_\parallel+\mathbf{q}_\parallel}-\varepsilon_{\mathbf{k}_\parallel})\,\left[\boldsymbol{q}_\parallel\otimes\boldsymbol{q}_\parallel^T\right]$$
$$= \frac{4n_ik_F^3}{\pi^2\hbar^2v_F\rho_0}\int\limits_{-\pi}^{\pi}d\beta_s\,|\cos\theta|\cos^2\theta\left|\frac{U_0^\tau(2k_F|\cos\theta|)}{\epsilon_\phi^2(2k_F|\cos\theta|)}\right|^2|\mathcal{F}_{\tau,\phi}(k_F,\beta_s)|^2$$
$$\times\left[\begin{array}{cc}\cos^2\theta & \cos\theta\sin\theta \\ \sin\theta\cos\theta & \sin^2\theta\end{array}\right]\ , \tag{33}$$

where $\epsilon_\phi(q_\parallel)$ is the static dielectric function, the structure factor $|\mathcal{F}_{\tau,\phi}(k_F,\beta_s)|^2$ is given by Eq. (27), $\cos\theta = -\sin(|\beta_s|/2)$, $\sin\theta = {\rm sgn}(\beta_s)\,\cos(|\beta_s|/2)$ for $-\pi\leq\beta_s\leq\pi$, and ${\rm sgn}(x)$ is a sign function.

7. MOBILITY

From Eq. (44), we get the linear equations [32] with respect to center-of-mass wave vector $\boldsymbol{K}_0^{\tau,\phi} = (K_x^{\tau,\phi}, K_y^{\tau,\phi})$, yielding

$$b_{xx}(\tau,\phi)K_x^{\tau,\phi} + \left[b_{xy}(\tau,\phi) - \frac{q_0 v_F B_z}{\hbar k_F}\right] K_y^{\tau,\phi} = \frac{q_0}{\hbar}\, E_x \ , \tag{34}$$

$$\left[b_{yx}(\tau,\phi) + \frac{q_0 v_F B_z}{\hbar k_F}\right] K_x^{\tau,\phi} + b_{yy}(\tau,\phi)K_y^{\tau,\phi} = \frac{q_0}{\hbar}\, E_y \ , \tag{35}$$

where $\boldsymbol{B}_\perp = (0,0,B_z)$, $\boldsymbol{E}_\parallel = (E_x, E_y, 0)$, $q_0 = -e$, and we have formally written the matrix $\overleftrightarrow{\boldsymbol{\mathcal{T}}}_p^{-1}(\tau,\phi) \equiv \{b_{ij}(\tau,\phi)\}$ with $i,j = x,y$. The determinant $Det\{\overleftrightarrow{\boldsymbol{\mathcal{C}}}_{\tau,\phi}\}$ of the coefficient matrix in Eqs. (34) and (35) is

$$Det\{\overleftrightarrow{\boldsymbol{\mathcal{C}}}_{\tau,\phi}\} = b_{xx}(\tau,\phi)\, b_{yy}(\tau,\phi) - \left[b_{xy}(\tau,\phi) - \frac{q_0 v_F B_z}{\hbar k_F}\right]\left[b_{yx}(\tau,\phi) + \frac{q_0 v_F B_z}{\hbar k_F}\right] \ . \tag{36}$$

Defining the source vector $\boldsymbol{s}$ as

$$\boldsymbol{s} = \left[\begin{array}{c} q_0 E_x/\hbar \\ q_0 E_y/\hbar \end{array}\right] \ , \tag{37}$$

we rewrite the linear equations as a matrix form $\overleftrightarrow{\boldsymbol{\mathcal{C}}}_{\tau,\phi} \cdot \boldsymbol{K}_0^{\tau,\phi} = \boldsymbol{s}$ with the solution $\boldsymbol{K}_0^{\tau,\phi} = \overleftrightarrow{\boldsymbol{\mathcal{C}}}_{\tau,\phi}^{-1} \cdot \boldsymbol{s}$. Here, the solution $\boldsymbol{K}_0^{\tau,\phi} = (K_x^{\tau,\phi}, K_y^{\tau,\phi})$ with $j = x,y$ is found to be

$$K_j^{\tau,\phi} = \frac{Det\{\overleftrightarrow{\boldsymbol{\Delta}}_j^{\tau,\phi}\}}{Det\{\overleftrightarrow{\boldsymbol{\mathcal{C}}}_{\tau,\phi}\}} \ , \tag{38}$$

where

$$Det\{\overleftrightarrow{\boldsymbol{\Delta}}_1^{\tau,\phi}\} = \frac{q_0}{\hbar}\, E_x\, b_{yy}(\tau,\phi) - \frac{q_0}{\hbar}\, E_y \left[b_{xy}(\tau,\phi) - \frac{q_0 v_F B_z}{\hbar k_F}\right] \ , \tag{39}$$

$$Det\{\overleftrightarrow{\boldsymbol{\Delta}}_2^{\tau,\phi}\} = \frac{q_0}{\hbar}\, E_y\, b_{xx}(\tau,\phi) - \frac{q_0}{\hbar}\, E_x \left[b_{yx}(\tau,\phi) + \frac{q_0 v_F B_z}{\hbar k_F}\right] \ . \tag{40}$$

The mobility tensor $\overleftrightarrow{\boldsymbol{\mu}}_{\tau,\phi} = \{\mu_{ij}^{\tau,\phi}\}$ can be obtained from $\mu_{ij}^{\tau,\phi} = (v_F/k_F)\,(\partial K_i^{\tau,\phi}/\partial E_j)$.

8. ELECTRON TRANSPORT

For transport of electrons in doped two-dimensional (2D) α-T_3 lattices, we first write down the Boltzmann transport equation for electrons in a conduction band $\varepsilon(k_\|) = \hbar v_F k_\|$. Here, the distribution function $f_\tau(\boldsymbol{r}_\|, \boldsymbol{k}_\|; t)$ in position-momentum spaces is determined by [29]

$$\frac{\partial f_\tau(\boldsymbol{r}_\|, \boldsymbol{k}_\|; t)}{\partial t} + \left\langle \frac{d\boldsymbol{r}_\|(t)}{dt} \right\rangle_{\rm av} \cdot \boldsymbol{\nabla}_{\mathbf{r}_\|} f_\tau(\boldsymbol{r}_\|, \boldsymbol{k}_\|; t)$$
$$+ \left\langle \frac{d\boldsymbol{k}_\|(t)}{dt} \right\rangle_{\rm av} \cdot \boldsymbol{\nabla}_{\mathbf{k}_\|} f_\tau(\boldsymbol{r}_\|, \boldsymbol{k}_\|; t) = \left. \frac{\partial f_\tau(\boldsymbol{r}_\|, \boldsymbol{k}_\|; t)}{\partial t} \right|_{\rm coll} , \tag{41}$$

where $\tau = \pm 1$ correspond to two inequivalent valleys $\boldsymbol{K}$ and $\boldsymbol{K}'$, $\boldsymbol{r}_\| = (x, y)$ and $\boldsymbol{k}_\| = (k_x, k_y)$ are in-plane position and wave vector, respectively. The right-hand side of Eq. (41) represents a collision (coll) contribution to electrons from ionized impurities. For electrons, we get $\boldsymbol{v}(\boldsymbol{k}_\|) = (1/\hbar)\boldsymbol{\nabla}_{\mathbf{k}_\|}\varepsilon(k_\|) = (\boldsymbol{k}_\|/k_\|)\, v_F$ for their group velocities. Moreover, we find [30] $\langle d\boldsymbol{r}_\|(t)/dt\rangle_{\rm av} = \boldsymbol{v}(\boldsymbol{k}_\|) - d\overline{\boldsymbol{K}}_0(t)/dt \times \boldsymbol{\Omega}_\perp(\boldsymbol{k}_\|) \equiv \boldsymbol{v}^*(\boldsymbol{k}_\|, t)$, where $\boldsymbol{v}^*(\boldsymbol{k}_\|, t)$ includes the anomalous group velocity [26], $\overline{\boldsymbol{K}}_0(t)$ is the wave vector for center-of-mass motion, $\boldsymbol{\Omega}_\perp(\boldsymbol{k}_\|) = \boldsymbol{\nabla}_{\mathbf{k}_\|} \times \overline{\boldsymbol{R}}_0(\boldsymbol{k}_\|)$ is the Berry curvature, and $\overline{\boldsymbol{R}}_0(\boldsymbol{k}_\|) = \langle \boldsymbol{k}_\| | \hat{\boldsymbol{r}}_\| | \boldsymbol{k}_\| \rangle = \langle \boldsymbol{k}_\| | i\hat{\boldsymbol{\nabla}}_{\mathbf{k}_\|} | \boldsymbol{k}_\| \rangle$ is the Berry connection.[26] Furthermore, we introduce a Newton-type force equation [29] for the wave vector of electrons, leading to $\langle d\boldsymbol{k}_\|(t)/dt\rangle_{\rm av} = (1/\hbar)\langle \boldsymbol{F}_{\rm em}(\boldsymbol{k}_\|, t)\rangle_{\rm av} = -(e/\hbar)\left\langle \left[\boldsymbol{E}_\|(t) + \boldsymbol{v}(\boldsymbol{k}_\|) \times \boldsymbol{B}_\perp(t)\right] \right\rangle_{\rm av}$, where $\boldsymbol{E}_\|(t)$ and $\boldsymbol{B}_\perp(t)$ are applied electric and magnetic fields, and $\boldsymbol{F}_{\rm em}(\boldsymbol{k}_\|, t)$ is the electromagnetic force acting on an electron in the $|\boldsymbol{k}_\|\rangle$ state.

By using Eq. (41), the zeroth-order Boltzmann moment equation [31–34] can be obtained after summing over all $\boldsymbol{k}_\|$ states on both sides of the equation. Having ignored the inter-valley scattering, we find $\partial\rho/\partial t + \boldsymbol{\nabla}_{\mathbf{r}_\|} \cdot \boldsymbol{J} = 0$, where the electron number per area $\rho(\boldsymbol{r}_\|, t)$, and the number current per length $\boldsymbol{J}(\boldsymbol{r}_\|, t)$ as well, are defined by $\rho(\boldsymbol{r}_\|, t) = \frac{2}{\mathcal{S}} \sum\limits_{\tau, \mathbf{k}_\|} f_\tau(\boldsymbol{r}_\|, \boldsymbol{k}_\|; t)$ and $\boldsymbol{J}(\boldsymbol{r}_\|, t) = \frac{2}{\mathcal{S}} \sum\limits_{\tau, \mathbf{k}_\|} \boldsymbol{v}^*(\boldsymbol{k}_\|, t)\, f_\tau(\boldsymbol{r}_\|, \boldsymbol{k}_\|; t)$ with $\mathcal{S}$ being the sample area.

For the first-order Boltzmann moment equation, we require the Fermi kinetics.[31–34] Here, we introduce the following energy-relaxation-time approximation

$$\left. \frac{\partial f_\tau(\boldsymbol{r}_\|, \boldsymbol{k}_\|; t)}{\partial t} \right|_{\rm coll} = -\frac{f_\tau(\boldsymbol{r}_\|, \boldsymbol{k}_\|; t) - f_T^{(0)}[\varepsilon(k_\|)]}{\tau_\phi(\boldsymbol{k}_\|, \tau)} , \tag{42}$$

where $f_T^{(0)}(x) = \{1 + \exp[(x - u_0)/k_BT]\}^{-1}$ is the Fermi function for thermal-equilibrium electrons, T is the sample temperature, $u_0(T)$ is the chemical potential of electrons, and $\tau_\phi(\boldsymbol{k}_\|, \tau)$ is the energy-relaxation time for electrons in the $\boldsymbol{k}_\|$ state. The calculation of $\tau_\phi(\boldsymbol{k}_\|, \tau)$ is given in Sec. 5, and $u_0(T)$ is determined from $N_0 = \rho_0\mathcal{S} = 4\sum\limits_{\mathbf{k}_\|} f_T^{(0)}[\varepsilon(k_\|)]$, where N_0 and ρ_0 are the total number of electrons and the electron areal density. Applying Eq. (42) to Eq. (41), we find

$$f_\tau(\boldsymbol{r}_\|,\boldsymbol{k}_\|;t)+\bar{\tau}_\phi(T,\tau)\,\frac{\partial f_\tau(\boldsymbol{r}_\|,\boldsymbol{k}_\|;t)}{\partial t}\approx f_T^{(0)}[\varepsilon(k_\|)]\,-\frac{\bar{\tau}_\phi(T,\tau)}{\hbar}\,\langle\boldsymbol{F}_{\rm em}(\boldsymbol{k}_\|,t)\rangle\cdot\boldsymbol{\nabla}_{\mathbf{k}_\|}f_T^{(0)}[\varepsilon(k_\|)]$$

$$-\bar{\tau}_\phi(T,\tau)\,\boldsymbol{v}^*(\mathbf{k}_\|)\cdot\boldsymbol{\nabla}_{\mathbf{r}_\|}f_T^{(0)}[\varepsilon(k_\|)]=f_T^{(0)}[\varepsilon(\boldsymbol{k}_\|)]-\frac{\bar{\tau}_\phi(T,\tau)}{\hbar}\langle\boldsymbol{F}(\boldsymbol{k}_\|,t)\rangle\cdot\boldsymbol{\nabla}_{\mathbf{k}_\|}f_T^{(0)}[\varepsilon(\boldsymbol{k}_\|)]\;, \qquad (43)$$

where T and u_0 are assumed spatially-uniform, and $1/\bar{\tau}_\phi(T,\tau)=\frac{2}{N_0}\sum\limits_{\mathbf{k}_\|}\frac{f_T^{(0)}[\varepsilon(k_\|)]}{\tau_\phi(\boldsymbol{k}_\|,\tau)}$. Making use of an inverse momentum-relaxation-time tensor $\overleftrightarrow{\boldsymbol{\mathcal{T}}}_p^{-1}(\tau,\phi)$, under the steady-state condition we rewrite the force-balance equation [35] with respect to the macroscopic center-of-mass wave vector $\boldsymbol{K}_0^{\tau,\phi}(t)$ as

$$\frac{d\boldsymbol{K}_0^{\tau,\phi}(t)}{dt}=-\overleftrightarrow{\boldsymbol{\mathcal{T}}}_p^{-1}(\tau,\phi)\cdot\boldsymbol{K}_0^{\tau,\phi}(t)+\frac{1}{\hbar}\,\boldsymbol{F}_{\tau,\phi}(t)$$

$$=-\overleftrightarrow{\boldsymbol{\mathcal{T}}}_p^{-1}(\tau,\phi)\cdot\boldsymbol{K}_0^{\tau,\phi}(t)-\frac{e}{\hbar}\,\left\{\boldsymbol{E}_\|(t)+\left(\frac{v_F}{k_F}\right)\boldsymbol{K}_0^{\tau,\phi}(t)\times\boldsymbol{B}_\perp(t)\right\}=0\;, \qquad (44)$$

where $\boldsymbol{F}_{\tau,\phi}(t)\equiv\langle\boldsymbol{F}_{\rm em}(\boldsymbol{k}_\|,t)\rangle_{\rm av}=-e\left\{\boldsymbol{E}_\|(t)+(v_F/k_F)\,\boldsymbol{K}_0^{\tau,\phi}(t)\times\boldsymbol{B}_\perp(t)\right\}$ is the macroscopic electromagnetic force, and $k_F=\sqrt{\pi\rho_0}$ is the Fermi wave number. The calculation of $\overleftrightarrow{\boldsymbol{\mathcal{T}}}_p^{-1}(\tau,\phi)$ can be found from SEc. 6. Equation (44) leads to $\boldsymbol{K}_0^{\tau,\phi}(t)=(k_F/v_F)\,\overleftrightarrow{\boldsymbol{\mu}}_{\tau,\phi}(\boldsymbol{B}_\perp(t),\,\overleftrightarrow{\boldsymbol{\mathcal{T}}}_p^{-1})\cdot\boldsymbol{E}_\|(t)$, where $\overleftrightarrow{\boldsymbol{\mu}}_{\tau,\phi}(\boldsymbol{B}_\perp,\,\overleftrightarrow{\boldsymbol{\mathcal{T}}}_p^{-1})$ is the electron mobility tensor. The calculation of the mobility tensor $\overleftrightarrow{\boldsymbol{\mu}}_{\tau,\phi}(\boldsymbol{B}_\perp,\,\overleftrightarrow{\boldsymbol{\mathcal{T}}}_p^{-1})$ are shown in Sec. 7. Using $\overleftrightarrow{\boldsymbol{\mu}}_{\tau,\phi}(\boldsymbol{B}_\perp,\,\overleftrightarrow{\boldsymbol{\mathcal{T}}}_p^{-1})$, we find $\boldsymbol{F}_{\tau,\phi}(t)=(\hbar k_F/v_F)\,\overleftrightarrow{\boldsymbol{\mathcal{T}}}_p^{-1}(\tau,\phi)\cdot\left\{\overleftrightarrow{\boldsymbol{\mu}}_{\tau,\phi}(\boldsymbol{B}_\perp(t),\,\overleftrightarrow{\boldsymbol{\mathcal{T}}}_p^{-1})\cdot\boldsymbol{E}_\|(t)\right\}$.

Similarly, multiplying both sides of Eq. (43) by $\boldsymbol{v}^*(\boldsymbol{k}_\|,t)$ and summing over all electron $\boldsymbol{k}_\|$ states afterwards, we find

$$\boldsymbol{J}_{\tau,\phi}(t)+\bar{\tau}_\phi(T,\tau)\,\frac{\partial\boldsymbol{J}_{\tau,\phi}(t)}{\partial t}=\frac{2}{\mathcal{S}}\,\sum_{\mathbf{k}_\|}\,\boldsymbol{v}^*(\boldsymbol{k}_\|,t)\,f_T^{(0)}[\varepsilon(k_\|)]$$

$$-\bar{\tau}_\phi(T,\tau)\,\frac{2}{\mathcal{S}}\,\sum_{\mathbf{k}_\|}\,\boldsymbol{v}^*(\boldsymbol{k}_\|,t)\left[\boldsymbol{F}_{\tau,\phi}(t)\cdot\boldsymbol{v}(\boldsymbol{k}_\|)\right]\,\frac{\partial f_T^{(0)}[\varepsilon(k_\|)]}{\partial\varepsilon}$$

$$=\frac{2e}{\hbar\mathcal{S}}\,\sum_{\mathbf{k}_\|}\,\left\{\left[\boldsymbol{E}_\|(t)+\left(\overleftrightarrow{\boldsymbol{\mu}}_{\tau,\phi}(\boldsymbol{B}_\perp(t),\,\overleftrightarrow{\boldsymbol{\mathcal{T}}}_p^{-1})\cdot\boldsymbol{E}_\|(t)\right)\times\boldsymbol{B}_\perp(t)\right]\times\boldsymbol{\Omega}_\perp(\boldsymbol{k}_\|)\right\}\,f_T^{(0)}[\varepsilon(k_\|)]$$

$$+\bar{\tau}_\phi(T,\tau)\,\left(\frac{\hbar k_F}{v_F}\right)\,\frac{2}{\mathcal{S}}\,\sum_{\mathbf{k}_\|}\,\boldsymbol{v}(\boldsymbol{k}_\|)$$

$$\times\left\{\overleftrightarrow{\boldsymbol{\mathcal{T}}}_p^{-1}(\tau,\phi)\cdot\left[\overleftrightarrow{\boldsymbol{\mu}}_{\tau,\phi}(\boldsymbol{B}_\perp(t),\,\overleftrightarrow{\boldsymbol{\mathcal{T}}}_p^{-1})\cdot\boldsymbol{E}_\|(t)\right]\right\}\cdot\boldsymbol{v}(\boldsymbol{k}_\|)\left\{-\frac{\partial f_T^{(0)}[\varepsilon(k_\|)]}{\partial\varepsilon}\right\}\;, \qquad (45)$$

where the second term on the left-hand side of the equation represents the non-adiabatic correction to the macroscopic number current per length $\boldsymbol{J}_{\tau,\phi}(t)$.

If $k_BT \ll E_F$ is low and external fields are assumed static, we obtain from Eq. (45) the total charge $(-e)$ current $\boldsymbol{j}(\tau,\phi) = \boldsymbol{j}_1(\tau,\phi) + \boldsymbol{j}_2(\tau,\phi)$ per length, where $E_F = \hbar v_F k_F$ is the electron Fermi energy. Explicitly, we have

$$\boldsymbol{j}_1(\tau,\phi) = -\frac{ek_F^2\bar{\tau}_\phi(k_F,\tau)}{2\pi^2 v_F^2}\int_0^{2\pi} d\theta_{\mathbf{k}_\parallel}\,\boldsymbol{v}(\theta_{\mathbf{k}_\parallel})\left\{\boldsymbol{\mathcal{T}}_p^{-1}(k_F,\tau,\phi)\cdot\left[\overleftrightarrow{\boldsymbol{\mu}}_{\tau,\phi}(\boldsymbol{B}_0^\perp,\,\overleftrightarrow{\boldsymbol{\mathcal{T}}}_p^{-1})\cdot\boldsymbol{E}_0^\parallel\right]\right\}\cdot\boldsymbol{v}(\theta_{\mathbf{k}_\parallel})$$

$$= -\frac{ek_F^2\bar{\tau}_\phi(k_F,\tau)}{2\pi}\int_{-\pi}^{\pi} d\beta_s\left[\hat{\boldsymbol{e}}_x\mathcal{C}_x(k_F,\tau,\phi,\beta_s)+\hat{\boldsymbol{e}}_y\mathcal{C}_y(k_F,\tau,\phi,\beta_s)\right] \equiv \int_{-\pi}^{\pi} d\beta_s\,\tilde{\boldsymbol{j}}_1(\tau,\phi,\beta_s)\ , \qquad (46)$$

which is mediated by the Lorentz force in position space, and

$$\boldsymbol{j}_2(\tau,\phi) = -\frac{e^2}{2\pi^2\hbar}\int d^2\boldsymbol{k}_\parallel\,\Theta(k_F-k_\parallel)\ \left\{\left[\boldsymbol{E}_0^\parallel+\left(\overleftrightarrow{\boldsymbol{\mu}}_{\tau,\phi}(\boldsymbol{B}_0^\perp,\,\overleftrightarrow{\boldsymbol{\mathcal{T}}}_p^{-1})\cdot\boldsymbol{E}_0^\parallel\right)\times\boldsymbol{B}_0^\perp\right]\times\boldsymbol{\Omega}_\perp(\boldsymbol{k}_\parallel)\right\}$$

$$= -\frac{e^2}{2\pi^2\hbar}\int d^2\boldsymbol{k}_\parallel\,\Theta(k_F-k_\parallel)\ \left\{\hat{\boldsymbol{e}}_x\left[E_y - B_z\left(\mu_{xx}(k_F,\tau,\phi)\,E_x+\mu_{xy}(k_F,\tau,\phi)\,E_y\right)\right]\,\Omega_{\tau,\phi}(\boldsymbol{k}_\parallel)\right.$$

$$\left.-\hat{\boldsymbol{e}}_y\left[E_x + B_z\left(\mu_{yx}(k_F,\tau,\phi)\,E_x+\mu_{yy}(k_F,\tau,\phi)\,E_y\right)\right]\,\Omega_{\tau,\phi}(\boldsymbol{k}_\parallel)\right\}$$

$$= -\frac{e^2}{2\pi^2\hbar}\left\{\frac{\tau(1-\alpha^2)\pi}{1+\alpha^2}\right\}\left\{\hat{\boldsymbol{e}}_x\left[E_y - B_z\left(\mu_{xx}(k_F,\tau,\phi)\,E_x+\mu_{xy}(k_F,\tau,\phi)\,E_y\right)\right]\right.$$

$$\left.-\hat{\boldsymbol{e}}_y\left[E_x + B_z\left(\mu_{yx}(k_F,\tau,\phi)\,E_x+\mu_{yy}(k_F,\tau,\phi)\,E_y\right)\right]\right\} \equiv j_{2x}(\tau,\phi)\,\hat{\boldsymbol{e}}_x + j_{2y}(\tau,\phi)\,\hat{\boldsymbol{e}}_y\ , \qquad (47)$$

which is mediated by the Berry curvature (or Berry force) in momentum space. Here, $\Theta(x)$ is a Heaviside step function, $\mu_{ij}(k_F,\tau,\phi)$ are four elements of the mobility tensor $\overleftrightarrow{\boldsymbol{\mu}}(k_F,\tau,\phi)$ in Eq. (53), $\boldsymbol{\Omega}_\perp(\boldsymbol{k}_\parallel) = \Omega_{\tau,\phi}(\boldsymbol{k}_\parallel)\,\hat{\boldsymbol{e}}_z$, $\Omega_{\tau,\phi}(\boldsymbol{k}_\parallel) = [\tau(1-\alpha^2)\pi/(1+\alpha^2)]\delta(\boldsymbol{k}_\parallel)$, $\alpha = \tan\phi$, $\theta_{\mathbf{k}_\parallel} = \tan^{-1}(k_y/k_x)$, $\boldsymbol{v}(\theta_{\mathbf{k}_\parallel}) = v_F(\cos\theta_{\mathbf{k}_\parallel},\,\sin\theta_{\mathbf{k}_\parallel})$, and $\hat{\boldsymbol{e}}_x$, $\hat{\boldsymbol{e}}_y$, $\hat{\boldsymbol{e}}_z$ are three unit coordinate vectors. $\tilde{\boldsymbol{j}}_1(\tau,\phi,\beta_s)$ in Eq. (46) is the non-equilibrium scattering current along the direction of a scattering angle β_s, which is τ dependent, while $\boldsymbol{j}_2(\tau,\phi)$ in Eq. (47) is the β_s-independent anomalous thermal-equilibrium current under doping ($E_F > 0$). We have also denoted $\mathcal{C}_{x,y}(k_F,\tau,\phi,\beta_s)$ as two spatial components of the vector $\boldsymbol{\mathcal{C}}(k_F,\tau,\phi,\beta_s) = \overleftrightarrow{\boldsymbol{\mathcal{T}}}_p^{-1}(k_F,\tau,\phi,\beta_s)\cdot\left\{\overleftrightarrow{\boldsymbol{\mu}}(k_F,\tau,\phi)\cdot\boldsymbol{E}_0^\parallel\right\}$ in Eq. (46).

The elements of a conductivity tensor $\overleftrightarrow{\boldsymbol{\sigma}}(\tau,\phi,\beta_s)$ are given by $\sigma_{ij}(\tau,\phi,\beta_s) = \tilde{\boldsymbol{j}}_1(\tau,\phi,\beta_s)\cdot\hat{\boldsymbol{e}}_i/(\boldsymbol{E}_0^\parallel\cdot\hat{\boldsymbol{e}}_j)$. From Eq. (46), we know $\overleftrightarrow{\boldsymbol{\sigma}}(\tau,\phi,\beta_s)$ depends on the mobility tensor, conduction-band energy dispersion and how electrons are distributed within the conduction band. To highlight scattering dynamics, we study the longitudinal $j_L(\tau,\phi)$ and transverse $j_T(\tau,\phi)$ currents flowing along and perpendicular to the direction of β_s, which are given by

$$
\begin{bmatrix} j_L(\tau,\phi) \\ j_T(\tau,\phi) \end{bmatrix} \equiv \int\limits_{-\pi}^{\pi} d\beta_s \begin{bmatrix} j_L(\tau,\phi,\beta_s) \\ j_T(\tau,\phi,\beta_s) \end{bmatrix} = -\frac{ek_F^2\bar{\tau}_\phi(k_F,\tau)}{2\pi} \int\limits_{-\pi}^{\pi} d\beta_s\, \mathcal{C}_x(k_F,\tau,\phi,\beta_s) \begin{bmatrix} \cos\beta_s \\ \sin\beta_s \end{bmatrix}
$$

$$
-\frac{ek_F^2\bar{\tau}_\phi(k_F,\tau)}{2\pi} \int\limits_{-\pi}^{\pi} d\beta_s\, \mathcal{C}_y(k_F,\tau,\phi,\beta_s) \begin{bmatrix} \sin\beta_s \\ -\cos\beta_s \end{bmatrix} , \tag{48}
$$

where the terms containing $\cos\beta_s$ select out the diagonal elements of $\overleftrightarrow{\mathcal{T}}_p^{-1}(k_F,\tau,\phi,\beta_s)$ in Eq. (51), while those containing $\sin\beta_s$ keep only the off-diagonal elements of $\overleftrightarrow{\mathcal{T}}_p^{-1}(k_F,\tau,\phi,\beta_s)$.

As $k_BT \ll E_F$, from Eq. (30) $\bar{\tau}_\phi(k_F,\tau)$ n Eq. (46) is calculated as

$$
\frac{1}{\bar{\tau}_\phi(k_F,\tau)} = \frac{4}{\rho_0\mathcal{S}} \sum_{\mathbf{k}_\parallel} \mathcal{W}_{\rm in}^{\tau,\phi}(k_\parallel)\Theta(k_F-|\boldsymbol{k}_\parallel|)
$$

$$
= \frac{4n_i}{\pi^2\hbar^2 v_F\rho_0} \int\limits_{-\pi}^{\pi} d\beta_s\, |\cos\theta| \int\limits_{0}^{k_F} dk_\parallel\, k_\parallel^2 \left| \frac{U_0^\tau(2k_\parallel|\cos\theta|)}{\epsilon_\phi(2k_\parallel|\cos\theta|)} \right|^2 |\mathcal{F}_{\tau,\phi}(k_\parallel,\beta_s)|^2 , \tag{49}
$$

which is valley dependent, where $0 \leq \phi < \pi/4$, $|\cos\theta| = |\sin(\beta_s/2)|$, $n_i = N_i/\mathcal{S}$ is the areal density of ionized impurities, and $\epsilon_\phi(q_\parallel)$ is the static dielectric function presented in Eqs. (15) and (16). The scattering form factor in Eq. (49) is given by

$$
\mathcal{F}_{\tau,\phi}(k_\parallel,\beta_s) = \frac{1}{2} \sum_{\ell} \left\{ (-i)^{-\tau}\tau\cos\phi\, \chi_{1,\ell}^\tau(k_\parallel) + \chi_{2,\ell}^\tau(k_\parallel) + (-i)^\tau\tau\sin\phi\, \chi_{3,\ell}^\tau(k_\parallel) \right\}
$$

$$
\times \left\{ (-i)^\tau\tau\cos\phi\, \chi_{1,\ell}^\tau(k_\parallel)\, e^{i\tau\beta^s_{\mathbf{k}_\parallel,\mathbf{q}_\parallel}} - \chi_{2,\ell}^\tau(k_\parallel) + (-i)^{-\tau}\tau\sin\phi\, \chi_{3,\ell}^\tau(k_\parallel)\, e^{-i\tau\beta^s_{\mathbf{k}_\parallel,\mathbf{q}_\parallel}} \right\}
$$

$$
\equiv \kappa_0(k_\parallel,\phi,\tau) + \kappa_1(k_\parallel,\phi,\tau)\, e^{i\tau\beta_s} + \kappa_2(k_\parallel,\phi,\tau)\, e^{-i\tau\beta_s} + \kappa_3(k_\parallel,\phi,\tau)(1+e^{i\tau\beta_s})
$$

$$
+\kappa_4(k_\parallel,\phi,\tau)(1+e^{-i\tau\beta_s}) + \kappa_5(k_\parallel,\phi,\tau)\cos(\tau\beta_s) , \tag{50}
$$

where $\chi_{n,\ell}^\tau(k_\parallel)$ with $n = 1, 2, 3$ are the complex scattering factors defined in Eq. (28), and six real scattering coefficients κ_j with $j = 0, 1, \cdots, 5$ are presented in Eq. (29).

The inverse momentum-relaxation-time tensor in Eq. (46) can be calculated from Eq. (33) under $k_BT \ll E_F$ as

$$
\overleftrightarrow{\mathcal{T}}_p^{-1}(k_F,\tau,\phi) = \frac{2\pi n_i}{\rho_0} \left(\frac{v_F}{k_F}\right) \sum_{\mathbf{k}_\parallel,\mathbf{q}_\parallel} \left| U_{\rm im}^{\tau,\phi}(\boldsymbol{q}_\parallel,\boldsymbol{k}_\parallel) \right|^2 \delta(\varepsilon_{\mathbf{k}_\parallel}-E_F)\, \delta(\varepsilon_{\mathbf{k}_\parallel+\mathbf{q}_\parallel}-\varepsilon_{\mathbf{k}_\parallel}) \left[\boldsymbol{q}_\parallel \otimes \boldsymbol{q}_\parallel^T\right]
$$

$$
= \frac{2n_ik_F^3}{\pi^2\hbar^2 v_F\rho_0} \int\limits_{-\pi}^{\pi} d\beta_s\, |\sin(\beta_s/2)| \sin^2(\beta_s/2) \left| \frac{U_0^\tau(2k_F|\sin(\beta_s/2)|)}{\epsilon_\phi(2k_F|\sin(\beta_s/2)|)} \right|^2 |\mathcal{F}_{\tau,\phi}(k_F,\beta_s)|^2
$$

$$\times \left[\begin{array}{cc} \sin^2(\beta_s/2) & -\sin(\beta_s)/2 \\ -\sin(\beta_s)/2 & \cos^2(\beta_s/2) \end{array}\right] \equiv \int_{-\pi}^{\pi} d\beta_s \, \overleftrightarrow{\boldsymbol{\mathcal{T}}}_p^{-1}(k_F,\tau,\phi,\beta_s) \; . \tag{51}$$

Here, the off-diagonal elements of $\overleftrightarrow{\boldsymbol{\mathcal{T}}}_p^{-1}(k_F,\tau,\phi)$ become zero after performing the integral with respect to β_s. On the other hand, the diagonal elements of $\overleftrightarrow{\boldsymbol{\mathcal{T}}}_p^{-1}(k_F,\tau,\phi)$ are kept nonzero and different. The diagonal elements of $\overleftrightarrow{\boldsymbol{\mathcal{T}}}_p^{-1}(k_F,\tau,\phi,\beta_s)$ are associated with the case in which directions of the scattering force and center-of-mass momentum are parallel to each other. The off-diagonal elements of $\overleftrightarrow{\boldsymbol{\mathcal{T}}}_p^{-1}(k_F,\tau,\phi,\beta_s)$, however, are connected to a situation where the directions of the scattering force and center-of-mass momentum are perpendicular to each other.

By writing $\overleftrightarrow{\boldsymbol{\mathcal{T}}}_p^{-1}(k_F,\tau,\phi)$ as

$$\overleftrightarrow{\boldsymbol{\mathcal{T}}}_p^{-1}(k_F,\tau,\phi) = \left[\begin{array}{cc} b_{xx}(k_F,\tau,\phi) & 0 \\ 0 & b_{yy}(k_F,\tau,\phi) \end{array}\right] \; , \tag{52}$$

$\overleftrightarrow{\boldsymbol{\mu}}(k_F,\tau,\phi)$ in Eq. (46) can be calculated from Eqs. (36), (38)-(40), and from $\mu_{ij}(k_F,\tau,\phi) = (v_F/k_F)\, \partial K_i^{\tau,\phi}/\partial E_j$ as well, and becomes

$$\overleftrightarrow{\boldsymbol{\mu}}(k_F,\tau,\phi) = \frac{-\frac{ev_F}{\hbar k_F}}{b_{xx}(k_F,\tau,\phi)\, b_{yy}(k_F,\tau,\phi) + \left(\frac{ev_F B_z}{\hbar k_F}\right)^2}$$

$$\times \left[\begin{array}{cc} b_{yy}(k_F,\tau,\phi) & -\frac{ev_F B_z}{\hbar k_F} \\ \frac{ev_F B_z}{\hbar k_F} & b_{xx}(k_F,\tau,\phi) \end{array}\right] \; , \tag{53}$$

which depends on τ and ϕ, where $\boldsymbol{B}_0^{\perp} = (0,0,B_z)$ leads to a normal Hall mobility.

From Eq. (53), we find $\boldsymbol{\mathcal{C}}(k_F,\tau,\phi,\beta_s) = (\mathcal{C}_x,\mathcal{C}_y) = \overleftrightarrow{\boldsymbol{\mathcal{T}}}_p^{-1}(k_F,\tau,\phi,\beta_s) \cdot \left[\overleftrightarrow{\boldsymbol{\mu}}(k_F,\tau,\phi) \cdot \boldsymbol{E}_0^{\parallel}\right]$ in Eq. (46) to be

$$\mathcal{C}_x(k_F,\tau,\phi,\beta_s) = -\left(\frac{ev_F}{\hbar k_F}\right) \left\{ \frac{b_{yy}(k_F,\tau,\phi)E_x - \left(\frac{ev_F B_z}{\hbar k_F}\right)E_y}{b_{xx}(k_F,\tau,\phi)\, b_{yy}(k_F,\tau,\phi) + \left(\frac{ev_F B_z}{\hbar k_F}\right)^2} \right\} d_{xx}(k_F,\tau,\phi,\beta_s)$$

$$-\left(\frac{ev_F}{\hbar k_F}\right) \left\{ \frac{\left(\frac{ev_F B_z}{\hbar k_F}\right)E_x + b_{xx}(k_F,\tau,\phi)E_y}{b_{xx}(k_F,\tau,\phi)\, b_{yy}(k_F,\tau,\phi) + \left(\frac{ev_F B_z}{\hbar k_F}\right)^2} \right\} d_{xy}(k_F,\tau,\phi,\beta_s) \; , \tag{54}$$

$$\mathcal{C}_y(k_F,\tau,\phi,\beta_s) = -\left(\frac{ev_F}{\hbar k_F}\right) \left\{ \frac{\left(\frac{ev_F B_z}{\hbar k_F}\right)E_x + b_{xx}(k_F,\tau,\phi)E_y}{b_{xx}(k_F,\tau,\phi)\, b_{yy}(k_F,\tau,\phi) + \left(\frac{ev_F B_z}{\hbar k_F}\right)^2} \right\} d_{yy}(k_F,\tau,\phi,\beta_s)$$

$$-\left(\frac{ev_F}{\hbar k_F}\right)\left\{\frac{b_{yy}(k_F,\tau,\phi)E_x-\left(\frac{ev_FB_z}{\hbar k_F}\right)E_y}{b_{xx}(k_F,\tau,\phi)\,b_{yy}(k_F,\tau,\phi)+\left(\frac{ev_FB_z}{\hbar k_F}\right)^2}\right\}d_{xy}(k_F,\tau,\phi,\beta_s)\ , \qquad (55)$$

where $\boldsymbol{E}_0^{\parallel}=(E_x,E_y,0)$ is assumed. Moreover, d_{xx}, d_{yy}, d_{xy} in Eq. (55) are calculated as

$$\begin{aligned}
d_{xx}(k_F,\tau,\phi,\beta_s) &= \mathcal{G}_s(k_F,\tau,\phi,\beta_s)\,(1-\cos\beta_s)\ ,\\
d_{yy}(k_F,\tau,\phi,\beta_s) &= \mathcal{G}_s(k_F,\tau,\phi,\beta_s)\,(1+\cos\beta_s)\ ,\\
d_{xy}(k_F,\tau,\phi,\beta_s) &= -\mathcal{G}_s(k_F,\tau,\phi,\beta_s)\,\sin\beta_s\ ,
\end{aligned} \qquad (56)$$

where the scattering function $\mathcal{G}_s(k_F,\tau,\phi,\beta_s)$ is defined as

$$\mathcal{G}_s(k_F,\tau,\phi,\beta_s)=\frac{n_ik_F^3}{4\pi^2\hbar^2v_F\rho_0}\left|\sin^3(\beta_s/2)\right|\left|\frac{U_0^\tau(2k_F|\sin(\beta_s/2)|)}{\epsilon_\phi(2k_F|\sin(\beta_s/2)|)}\right|^2|\mathcal{F}_{\tau,\phi}(k_F,\beta_s)|^2\ . \qquad (57)$$

Physically, the terms containing $d_{xy}(k_F,\tau,\phi,\beta_s)$ in Eqs. (54) and (55) represent the skew-scattering contributions.

9. RESULTS

The major parameters chosen for our numerical calculations are listed in Table 1. The other parameters, such as, ϕ, τ, B_z, will be given directly in figure captions.

We show in Fig. 2 the β_s dependent $j_L(\tau,\phi,\beta_s)$ (a)-(b) and $j_T(\tau,\phi,\beta_s)$ (c)-(d) in Eq. (48) with various ϕ and B_z for $\tau=1$ $(a),(c)$ and $\tau=-1$ $(b),(d)$. From Figs. 2(a) and 2(b) we find a triplet peak for $j_L(\tau,\phi,\beta_s)$ in both $\beta_s>0$ and $\beta_s<0$ regions. We always see one backward plus one forward near-vertical (near-horizontal) scattering of electrons from two different valley impurities, characterized by $\tau=1$ $(\tau=-1)$. $j_L(\tau,\phi,\beta_s)$ for $\tau=1$ is about one order of magnitude larger than that for $\tau=-1$ because of a larger mobility for the barrier-like potential. Increasing B_z significantly reduces $j_L(\tau,\phi,\beta_s)$ at $\phi=\pi/6$ for both $\tau=\pm1$ (black and red) due to cyclotron motion. Meanwhile, increasing Berry phase ϕ further reduces $j_L(\tau,\phi,\beta_s)$ at $B_z/B_0=0.01$ for both $\tau=\pm1$ (red and blue) due to decreasing Berry force. Furthermore, we see the negative triplet peak for $j_T(\tau,\phi,\beta_s)$ in both $\beta_s>0$ and $\beta_s<0$ regions, as displayed in Figs. 2(c) and 2(d). $j_T(\tau,\phi,\beta_s)$ presents the same dependence as for the triplet peak in $j_L(\tau,\phi,\beta_s)$ on B_z and ϕ. In this case, however, one always finds a counter-clockwise tangential current $j_T(\tau,\phi,\beta_s)$ for dominant near-horizontal forward- and backward-scattering of electrons with an impurity at both valleys.

For a comparison with measurable currents, we display in Fig. 3 the calculated total back-scattering current $j_{1x}(\tau,\phi)$ in (a)-(b), and total skew-scattering current $j_{1y}(\tau,\phi)$ in (c)-(d) as well, in Eq. (46) as a function of B_z with various ϕ for $\tau=1$ (a), (c) and $\tau=-1$ (b), (d). From Figs. 3(a) and 3(b), we find a slow (fast) monotonic decrease of $j_{1x}(\tau,\phi)$ with increasing B_z in the scale of $\sim 1/B_z^2$ for $\tau=1$ $(\tau=-1)$ due to cyclotron motion. Such different behaviors result from higher (lower) longitudinal mobility at the $\tau = 1$ ($\tau = -1$) valley. However, increasing ϕ decreases $j_{1x}(\tau, \phi)$ for both $\tau = \pm 1$. For $j_{1y}(\tau, \phi)$ in Figs. 3(c) and 3(d), on the other hand, the same Lorentz force initially enhances $j_{1y}(\tau, \phi)$ dramatically for all values of ϕ and $\tau = \pm 1$ at very low B_z but eventually reduces $j_{1y}(\tau, \phi)$ slowly (quickly) for $\tau = 1$ ($\tau = -1$) for large B_z (in the scale of $\sim 1/B_z$) due to cyclotron motion of electrons. This huge initial increase in $j_{1y}(\tau, \phi)$ at very low B_z, however, is greatly suppressed in graphene with the maximum Berry force at $\phi = 0$ (black). Therefore, a Berry-phase dependent asymmetry in suppressing the skew currents by electron cyclotron motion can be verified by a comparison of Figs. 3(c) with Fig. 3(d). For a gVHE, the Berry phase can be employed for mediating the VHE. In our case, an external magnetic field can be applied further to control this gVHE. Experimentally, one can measure both the back-scatter and the skew-scattering non-equilibrium electrical currents in Eq. (46) as a function of B_z using the standard van der Pauw method [36] so as to verify unique features associated with different ϕ at low B_z. In this case, however, the contributions from equilibrium longitudinal and Hall currents in Fig. 4 should be deducted from the corresponding total current measured.

At last, from Eq. (47) we know there exists another conduction current $\boldsymbol{j}_2(\tau, \phi)$ even in the thermal-equilibrium state due to Berry curvature $\boldsymbol{\Omega}_\perp(\boldsymbol{k}_\|)$, leading to the so-called anomalous Hall effect (AHE) as $\phi \neq \pi/4$. Figure 4 displays the calculated AHE current components $j_{2x}(\tau, \phi)$ in (a)-(b) and $j_{2y}(\tau, \phi)$ in (c)-(d). Since $\boldsymbol{j}_2(\tau, \phi)$ is proportional to τ, we expect the sign change in Figs. 4(a) and 4(b) for $j_{2x}(\tau, \phi)$ and in Figs. 4(c) and 4(d) for $j_{2y}(\tau, \phi)$. As an indication of gVHE, the increasing Berry force (or decreasing ϕ) in momentum space will slowly (quickly) enhance $j_{2x}(\tau, \phi)$ at small B_z and $j_{2y}(\tau, \phi)$ at $B_z = 0$ due to large (small) longitudinal mobility at $\tau = 1$ ($\tau = -1$). However, the AHE current is weakened by the Lorentz force (or increasing B_z) in position space for large B_z, where $j_{2x}(\tau, \phi)$ comes only from one term $\sim B_z \mu_{xx} E_x$, while $j_{2y}(\tau, \phi)$ is produced by two terms $\sim (1 + B_z \mu_{yx}) E_x$. As a result, $j_{2x}(\tau, \phi)$ decreases like $\sim 1/B_z$ in the high-field limit. Meanwhile, $j_{2y}(\tau, \phi)$ also approaches zero in the same strong-field limit but it scales as $\sim 1/B_z^2$. Since there are two orders of magnitude difference in μ_{xx} and μ_{yx} for $\tau = 1$ and -1, we expect the decrease in $j_{2x}(\tau, \phi)$ and $j_{2y}(\tau, \phi)$ to become much faster at the $\tau = -1$ valley, and therefore, a net AHE current (sum of currents from both valleys) exists and will be mainly decided by the $\tau = 1$ valley for large B_z. We can make use of the experimentally measured mobility tensor and Eq. (47) to independently quantify the Berry-curvature induced longitudinal and Hall currents as a function of perpendicular magnetic field B_z.

10. SUMMARY

In this paper, we have demonstrated the Berry-phase mediation to valley-dependent Hall transport in α-T_3 lattices. We analyze the observed interplay between the Lorentz force in position space and the Berry force in momentum space for the total sheet current density including both normal longitudinal and Hall currents as well as anomalous Hall current. We also incorporate many-body screening to electron-impurity interactions, which is crucial for avoiding overestimation of scattering. We further demonstrate triplet peak at two distinct valleys and in near-horizontal and near-vertical scattering directions for forward- and back-scattering current, which favor small Berry phases and low magnetic fields. We also present a magnetic-field dependence of both non-equilibrium and thermal-equilibrium currents from Berry-phase-mediated and valley-dependent longitudinal and transverse transport.

In our theory, we have employed the first two Boltzmann moment equations in calculations of scattering-angle dependence for extrinsic skew-scattering currents due to the presence of randomly-distributed impurities in α-T_3 lattices, where both energy- and momentum-relaxation times are computed microscopically. We attribute this scattering-angle dependence to an anisotropic inverse momentum-relaxation-time tensor calculated within the screened second-order Born approximation and using a static dielectric function within the random-phase approximation. Meanwhile, we also include the isotropic intrinsic current due to Berry curvature for electrons in thermal-equilibrium states. Under a perpendicular magnetic field, we observe an interplay by Lorentz and valley-dependent resistive forces acting on electrons, leading to field-dependent skew currents. We further find these skew currents can be mediated by Berry phases of α-T_3 lattices and depend on barrier- or trap-type impurity potentials at two inequivalent valleys.

ACKNOWLEDGEMENTS

DH would like to acknowledge the financial supports from the Laboratory University Collaboration Initiative (LUCI) program and from the Air Force Office of Scientific Research (AFOSR).

REFERENCES

1. S. D. Bader and S. S. P. Parkin, Ann. Rev. Condensed Matt. Phys. **1**, 71 (2010).
2. A. Rycerz, J. Tworzydlo, and C. W. J. Beenakker, Nat. Phys. **3**, 172 (2007).
3. D. Xiao, W. Yao, and Q. Niu, Phys. Rev. Lett. **99**, 236809 (2007).
4. K. Behnia, Nat. Nanotech. **7**, 488 (2012).
5. C. E. Nebel, Nat. Mater. **12**, 690 (2013).
6. R. V. Gorbachev, J. C. W. Song, G. L. Yu, A. V. Kretinin, F. Withers, Y. Cao, A. Mishchenko, I. V. Grigorieva, K. S. Novoselov, L. S. Levitov, and A. K. Geim, Science **346**, 448 (2014).
7. X. Xu, W. Yao, D. Xiao, and T. F. Heinz, Nat. Phys. **10**, 343 (2014), review.
8. A. Kundu, H. A. Fertig, and B. Seradjeh, Phys. Rev. Lett. **116**, 016802 (2016).
9. Y. Ye, J. Xiao, H.-L. Wang, Z.-L. Ye, H.-Y. Zhu, M. Zhao, Y. Wang, J.-H. Zhao, X.-B. Yin, and X. Zhang, Nat. Nanotech. **11**, 598 (2016).
10. J. Lu, C. Qiu, M. Ke, and Z. Liu, Phys. Rev. Lett. **116**, 093901 (2016).

11. F. Delgado and J. Fernández-Rossier, Phys. Rev. Lett. **108**, 196602 (2012).

12. K. S. Novoselov, A. K. Geim, et al, Sci. **306**, 666 (2004).

13. K. F. Mak, K. L. McGill, J. Park, and P. L. McEuen, Sci. **344**, 1489 (2014).

14. A. Rycerz, J. Tworzydlo and C. W. J. Beenakker, Nat. Phys. **3**, 172 (2007)

15. N. Nagaosa, J. Sinova, S. Onoda, A. H. MacDonald, and N. P. Ong, Rev. Mod. Phys. **82**, 1539 (2010).

16. J. Sinova, S. O. Valenzuela, J. Wunderlich, C.H. Back, and T. Jungwirth, Rev. Mod. Phys. **87**, 1213 (2015).

17. A. Raoux, M. Morigi, J.-N. Fuchs, F. Piéchon, and G. Montambaux, Phys. Rev. Lett. **112**, 026402 (2014).

18. J. D. Malcolm and E. J. Nicol, Phys. Rev. B **93**, 165433 (2016).

19. B. Dey and T. K. Ghosh, Phys. Rev. B **98**, 075422 (2018).

20. K. Novoselov, A. K. Geim, S. Morozov, D. Jiang, M. Katsnelson, I. Grigorieva, S. Dubonos, and A. Firsov, Nat. **438**, 197 (2005).

21. R. R. Nair, P. Blake, A. N. Grigorenko, K. S. Novoselov, T. J. Booth, T. Stauber, N. M. Peres, and A. K. Geim, Sci. **320**, 1308 (2008).

22. A. C. Ferrari, J. Meyer, V. Scardaci, C. Casiraghi, M. Lazzeri, F. Mauri, S. Piscanec, D. Jiang, K. Novoselov, S. Roth, et al., Phys. Rev. Lett. **97**, 187401 (2006).

23. H.-Y. Xu, L. Huang, D. H. Huang, and Y.-C. Lai, Phys. Rev. B **96**, 045412 (2017).

24. D. H. Huang, A. Iurov, H.-Y. Xu, Y.-C. Lai, and G. Gumbs, *Interplay of Lorentz-Berry forces in position-momentum spaces for valley-dependent impurity scattering in α-T_3 lattices* (to appear in Phys. Rev. B).

25. D. Moldovan, M. Ramezani Masir, L. Covaci, and F. M. Peeters, Phys. Rev. B **86**, 115431 (2012).

26. Q. Niu, M.-C. Chang, B. Wu, D, Xiao, and R. Cheng, *Physical Effects of Geometric Phases* (World Scientific Publishing Co. Pte. Ltd., Singapore, 2017)

27. D. H. Huang, A. Iurov, F. Gao, G. Gumbs and D. A. Cardimona, Phys. Rev. Appl. **9**, 024002 (2018).

28. G. Gumbs and D. H. Huang, *Properties of Interacting Low-Dimensional Systems* (Wiley-VCH Verlag GmbH & Co. KGaA, Boschstr, Weinheim, 2011).

29. J. M. Ziman, *Principles of the Theory of Solids* (2nd Ed., Cambridge University Press, 1972).

30. G. Sundaram and Q. Niu, Phys. Rev. B **59**, 14 915 (1999).

31. D. H. Huang, G. Gumbs and O. Roslyak, J. Mod. Opt. **58**, 1898 (2011).

32. D. Backes, D. H. Huang, R. Mansell, M. Lanius, J. Kampmeier, D. Ritchie, G. Mussler, G. Gumbs, D. Grützmacher, and V. Narayan, Phys. Rev. B **96**, 125125 (2017).

33. N. C. Miller, M. Grupen, K. Beckwith, D. Smithe, and J. D. Albrecht, J. Comput. Electr. **17**, 1658 (2018).

34. D. Backes, D. H. Huang, R. Mansell, M. Lanius, J. Kampmeier, D. Ritchie, G. Mussler, G. Gumbs, D. Grützmacher, and V. Narayan, Phys. Rev. B **99**, 125139 (2019).

35. D. H. Huang, P. M. Alsing, T. Apostolova and D. A. Cardimona, Phys. Rev. B **71**, 195205 (2005).

36. L. J. van der Pauw, Philips Res. Rep. **13**, 1 (1958).

Table 1. Parameters for Calculations

Parameter	Value (unit)
v_F	$5 \times 10^{11}\,\mathrm{cm}^{-2}$
k_F	$1.25 \times 10^{6}\,\mathrm{cm}^{-1}$
E_F	$130\,\mathrm{meV}$
n_i	$2.5 \times 10^{11}\,\mathrm{cm}^{-2}$
ϵ_r	13.0
V_0	$420\,\mathrm{meV}$
r_0	$560\,\mathrm{\AA}$
E_x	$0.5\,\mathrm{kV/cm}$
E_y	0

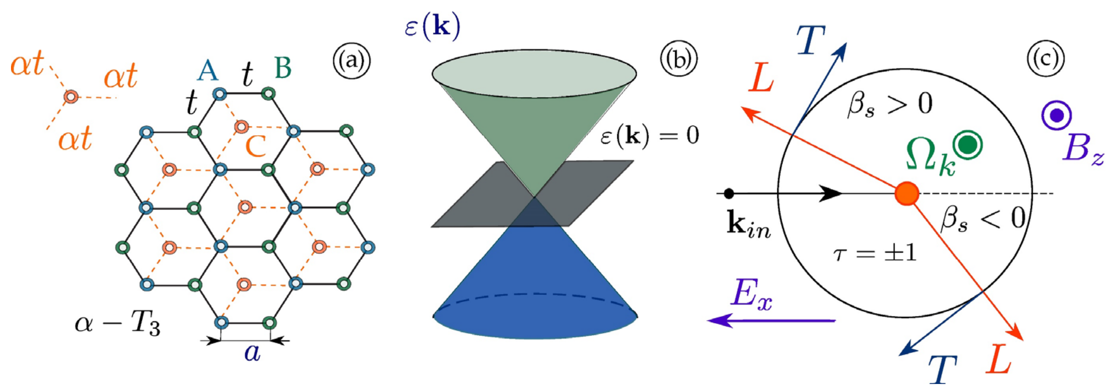

Figure 1. (a) α-T_3 lattice with three atoms (A, B, C) per unit cell within the xy-plane, where $\alpha = \tan\phi$ characterizes the ratio of the bonding strengths between A-C and A-B atoms; (b) illustration for three bands of α-T_3 lattice, including a flat middle one; (c) schematic for a scattering angle β_s of an incident electron with wave vector $\boldsymbol{k}_{\rm in}$ by impurities at two valleys characterized by $\tau = \pm 1$ under an electric field $\boldsymbol{E}_x$ in the x direction, where a magnetic field $\boldsymbol{B}_z$ and the Berry curvature $\boldsymbol{\Omega}_k$ are in the z direction and the longitudinal (transverse) scattering is labeled by L (T), respectively.

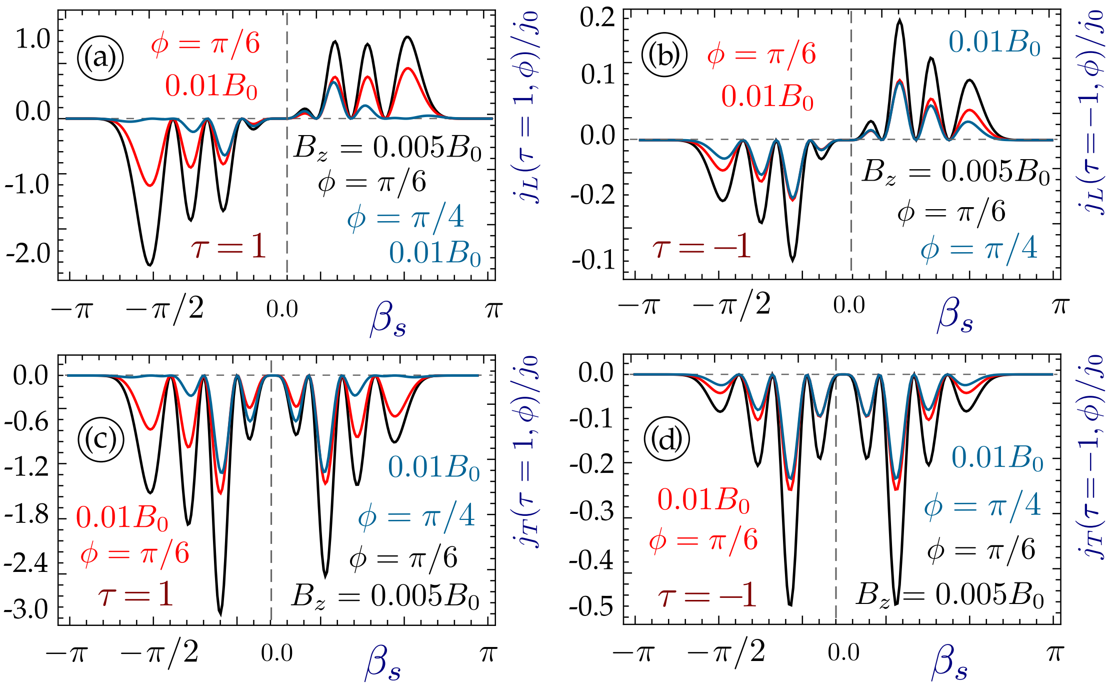

Figure 2. Calculated $j_L(\tau, \phi, \beta_s)$ (a)-(b) and $j_T(\tau, \phi, \beta_s)$ (c)-(d) in Eq. (48) as a function of β_s with $\phi = \pi/4$, $B_z/B_0 = 0.01$ (blue), $\phi = \pi/6$, $B_z/B_0 = 0.01$ (red) and $\phi = \pi/6$, $B_z/B_0 = 0.005$ (black) for $\tau = 1$ $(a), (c)$ and $\tau = -1$ $(b), (d)$. Here, $j_0 = n_i e v_F$ and $B_0 = \hbar k_F^2/e$.

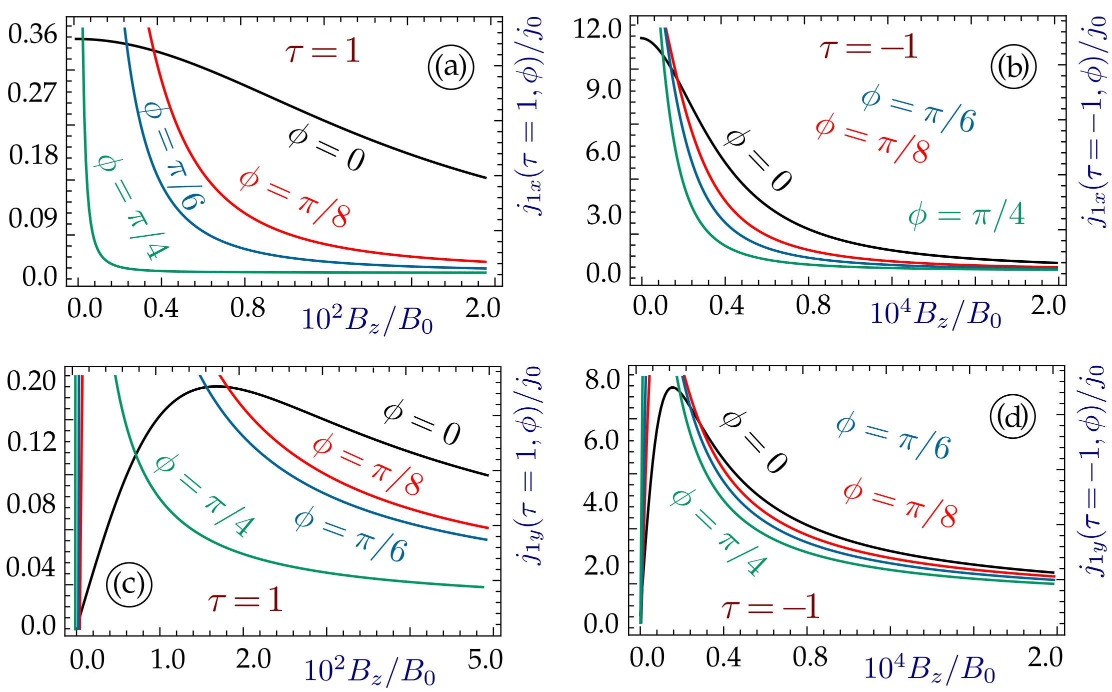

Figure 3. Calculated $j_{1x}(\tau, \phi)$ (a)-(b) and $j_{1y}(\tau, \phi)$ (c)-(d) in Eq. (46) as a function of B_z with $\phi = \pi/4$ (green), $\phi = \pi/6$ (blue), $\phi = \pi/8$ (red) and $\phi = 0$ (black) for $\tau = 1$ $(a), (c)$ and $\tau = -1$ $(b), (d)$. Here B_0 and j_0 are given in Fig. 2.

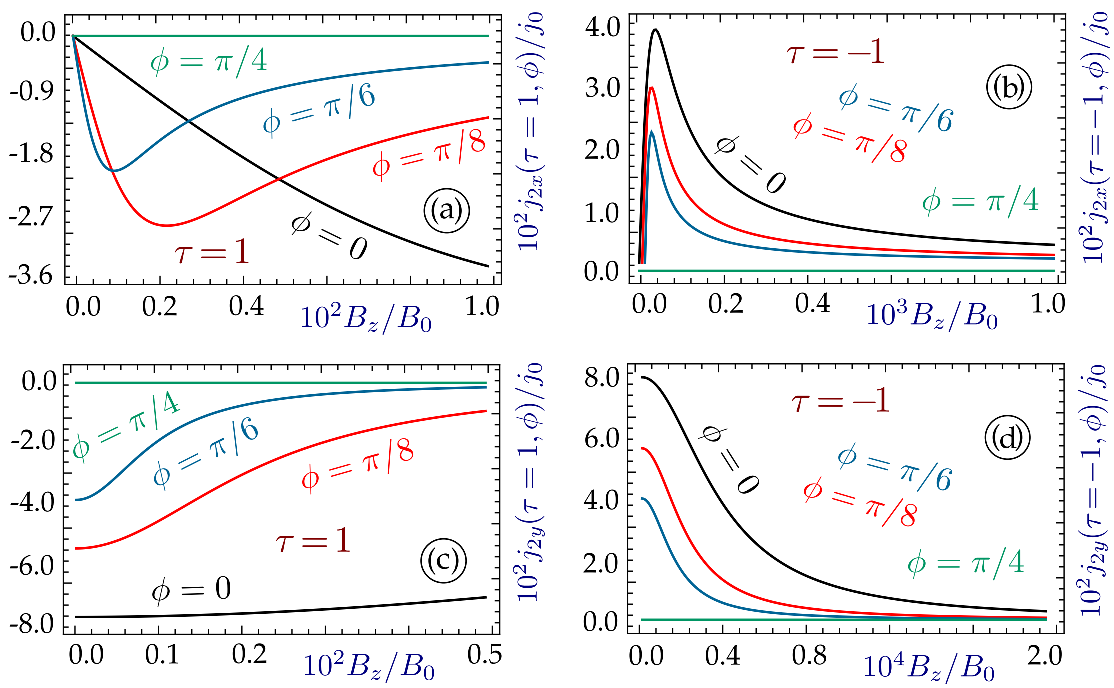

Figure 4. Calculated $j_{2x}(\tau, \phi)$ (a)-(b) and $j_{2y}(\tau, \phi)$ (c)-(d) fin Eq. (47) as a function of B_z with $\phi = \pi/4$ (green), $\phi = \pi/6$ (blue), $\phi = \pi/8$ (red) and $\phi = 0$ (black) for $\tau = 1$ $(a), (c)$ and $\tau = -1$ $(b), (d)$. Here B_0 and j_0 are given in Fig. 2.